2012

Continued Monitoring of Indiana's SPS9-A Site

Ayesha Shah
Purdue University, bano@purdue.edu

Rebecca S. McDaniel
Purdue University, rsmcdani@purdue.edu

Jan Olek
Purdue University, olek@purdue.edu

JOINT TRANSPORTATION RESEARCH PROGRAM

INDIANA DEPARTMENT OF TRANSPORTATION
AND PURDUE UNIVERSITY

CONTINUED MONITORING OF INDIANA'S SPS9-A SITE

Ayesha Shah
Research Engineer
North Central Superpave Center
Purdue University
Corresponding Author

Rebecca S. McDaniel
Technical Director
North Central Superpave Center
Purdue University

Jan Olek
Professor of Civil Engineering
School of Civil Engineering
Purdue University

SPR-3017
Report Number: FHWA/IN/JTRP-2012/19
DOI: 10.5703/1288284314983

RECOMMENDED CITATION

Shah, A., R. S. McDaniel, and J. Olek. *Continued Monitoring of Indiana's SPS9-A Site*. Publication FHWA/IN/JTRP-2012/19. Joint Transportation Research Program, Indiana Department of Transportation and Purdue University, West Lafayette, Indiana, 2012. doi: 10.5703/1288284314983.

CORRESPONDING AUTHOR

Ayesha Shah
North Central Superpave Center
Purdue University
(765) 463-2317, ext. 227
bano@purdue.edu

JOINT TRANSPORTATION RESEARCH PROGRAM

The Joint Transportation Research Program serves as a vehicle for INDOT collaboration with higher education institutions and industry in Indiana to facilitate innovation that results in continuous improvement in the planning, design, construction, operation, management and economic efficiency of the Indiana transportation infrastructure.
https://engineering.purdue.edu/JTRP/index_html

Published reports of the Joint Transportation Research Program are available at: http://docs.lib.purdue.edu/jtrp/

NOTICE

TECHNICAL REPORT STANDARD TITLE PAGE

1. Report No.	2. Government Accession No.	3. Recipient's Catalog No.
FHWA/IN/JTRP-2012/19		

4. Title and Subtitle	5. Report Date
Continued Monitoring of Indiana's SPS9-A Site	July 2012
	6. Performing Organization Code

7. Author(s)	8. Performing Organization Report No.
Ayesha Shah, Rebecca S. McDaniel and Jan Olek	FHWA/IN/JTRP-2012/19

9. Performing Organization Name and Address	10. Work Unit No. (TRAIS)
Joint Transportation Research Program Purdue University 550 Stadium Mall Drive West Lafayette, IN 47907-2051	**11. Contract or Grant No.** SPR-3017

12. Sponsoring Agency Name and Address	13. Type of Report and Period Covered
Indiana Department of Transportation State Office Building 100 North Senate Avenue Indianapolis, IN 46204	Final Report
	14. Sponsoring Agency Code

15. Supplementary Notes

Prepared in cooperation with the Indiana Department of Transportation and Federal Highway Administration.

16. Abstract

This study was initiated to continue monitoring the performance of five test sections placed in 1997 to compare the performance of Superpave asphalt mixtures with different binder grades and one test section designed using the Marshall mix design method. A previous study had evaluated the performance of these test sections for four years after construction. This study extended that evaluation period to 12 years. During that time period, cores were taken from each test section at 9.5 and 12 years in service. Cores were tested and analyzed to determine the volumetrics and low temperature cracking behavior of the mixtures. Additional cores were used to extract, recover and test the binder in the mixtures. Results showed that the air void content in the mixtures did continue to decrease up to about nine years then appears to have leveled off. Aging (stiffening) of the unmodified binders was observed through Dynamic Shear Rheometer testing of the recovered binders but not by the penetration test. The modified binder did not exhibit the same level of aging as the unmodified binders. Aging also affected the recovered low temperature binder grade of four of the six binders, but the other two seemed relatively insensitive to aging at low temperatures. Testing of field cores showed that all of the mixtures would be expected to show thermal cracking at 9.5 years and beyond; this was confirmed by field distress surveys. The mix with polymer modified binder showed the greatest amount of cracking, which began at an early age in the field; this was not expected and did not correlate well with the lab testing results for unknown reasons. The mix with 15% RAP was slightly stiffer than a companion control mix without RAP, but the difference in predicted cracking temperature was only 1 - 2°C for the surface mixes. Based on these results, INDOT can continue to use Superpave mixes with confidence, especially when considering the fact that Superpave has continued to evolve and be refined since this project was constructed. The mixture with RAP has performed about as well as the virgin mixtures under heavy interstate traffic.

17. Keywords	18. Distribution Statement
SPS9-A, long-term performance, pavement monitoring, recovered binders, transverse cracking, RAP section	No restrictions. This document is available to the public through the National Technical Information Service, Springfield, VA 22161.

19. Security Classif. (of this report)	20. Security Classif. (of this page)	21. No. of Pages	22. Price
Unclassified	Unclassified	40	

EXECUTIVE SUMMARY

CONTINUED MONITORING OF INDIANA'S SPS9-A SITE

Introduction

The Indiana's SPS9-A site was initiated as a part of the SHRP's LTPP program in 1997 to study the influence of binder grades on mixture performance. In the earlier phase of this study entitled *Development of Indiana's SPS9-A Site*, five Superpave sections with different binder grade as (including one SBS-modified binder) and one Marshall section were constructed on a 2.5-km section along eastbound I-70 east of Indianapolis. Four of the five Superpave mixes had the same aggregate gradation, source and mix design. The remaining fifth section contained 15% RAP and the same binder grade as the control Superpave section. In an earlier study, lab-compacted specimens from plant-produced mixtures obtained at the time of construction were tested to evaluate rutting and thermal cracking performance. Binders recovered from field core samples at predetermined intervals were tested. These results were compared with findings from field distress surveys conducted within the initial four-year study period. Discrepancies between the observed pavement distress (cracking and rutting) and mixture testing resulted in the initiation of the current study, with a view to obtain two more sets of field core samples for additional testing on recovered binders and for assessing the cracking resistance of the mixtures by directly testing the core samples at low temperatures. The overall objective of this research project was to provide long-term performance data of mixes with the same job-mix formula (JMF) and gradation but with different binder grades. It was also to allow evaluation of the long-term performance of RAP.

Findings

The air void content of the mixes in the field decreased from the time of construction through about 9.5 years, then remained relatively constant to 12 years. Aging of the binders in the mixtures was evidenced by increasing recovered binder high-temperature stiffness over time; the aging from 9.5 to 12 years was minimal. As time increased, the recovered low-temperature binder grade also increased (became warmer) for most of the binders, also indicating aging of the binder. Two of the binders were relatively insensitive to changes in the low-temperature grade with time. The binder data suggested that four of the six test sections would be expected to exhibit thermal cracking in the field. Low-temperature mixture testing indicated that all six test sections would show thermal cracking by 9.5 years and beyond. With the exception of the mix with polymer modified binder, the distress observed during field distress surveys correlated well with the laboratory binder and mixture test results. In general, mixes with the lower low-temperature grade showed better resistance to thermal cracking compared with mixes with higher low-temperature grade. The RAP section showed a slightly higher amount of total transverse cracking than the control mix. The section with the softest binder (PG58-28) had a minimal amount of low-temperature cracking at the end the final distress survey (6 years in service). Rutting was observed in all test sections at that time. The section with the SBS-modified binder showed the greatest amount of total crack length, contrary to expectations. No explanation for this behavior could be found from the test data.

Implementation

This long-term evaluation of the performance of Marshall and Superpave mixtures with different binders did not raise any "red flags" signifying cause for concern with the current binder grade selection policy or implementation of RAP in surface mixtures. The specification changes that have already been implemented were confirmed. No additional changes are required based on this research.

CONTENTS

LIST OF TABLES

LIST OF FIGURES

1. BACKGROUND AND EXPERIMENTAL PLAN

In the early 1990s, the Strategic Highway Research Program (SHRP) was beginning to yield products from its intensive research efforts. One of the key products that was coming into being at that time was the Superpave asphalt mix design system. Superpave comprised new binder specifications and tests, generally tighter aggregate requirements, a volumetric mix design protocol using a new gyratory compactor, and mixture tests that were intended to allow prediction of rutting and cracking over time. (The story of how Superpave was developed and implemented is described in *The Superpave Mix Design System: Anatomy of a Research Program* (*1*).)

In order to facilitate and encourage implementation of the new mix design system, an experiment was planned to place Superpave mixtures in the field to evaluate their performance and compare them to other mixtures. This experiment was part of the Long Term Pavement Performance (LTPP) program, the only part of SHRP that was to last for more than five years. The LTPP program included monitoring of existing pavement sections, called the General Pavement Studies (GPS), and construction and monitoring of new pavements to evaluate specific design features, called Special Pavement Studies (SPS). The evaluation of Superpave mixtures was a part of SPS-9, Validation of the SHRP Asphalt Specification and Mix Design (Superpave). The plan was to follow the performance of SPS-9 sites constructed around the country for up to 20 years as part of the overall LTPP program. While some monitoring was done by the LTPP Regional Contractor, the full extent of monitoring was not conducted, largely because of delays in passage of SAFETEA-LU, the federal transportation bill in 2005, and the budget cuts that were a part of that legislation.

The first pilot SPS-9 sites were designated SPS9-A. Indiana's SPS9-A site was constructed in 1997 on I-70 east of Indianapolis. The SHRP program had developed experimental plans for specific factors that needed to be evaluated on a national basis, but the program also allowed states to add test sections to evaluate additional features of interest. The construction and early performance of Indiana's SPS9-A site was documented under a previous JTRP project, SPR-2148, *Development of Indiana's SPS9-A Site* (*2*). This report summarizes the findings of an extended monitoring program on that site.

1.1 Experimental Plan

Indiana's SPS9-A study site consisted of an asphalt concrete (AC) overlay (surface and intermediate layers) placed over cracked and seated jointed reinforced concrete pavement (JRCP) that was used a base course, constructed along I-70. Five test sections were designed using Superpave mix design methodology and one section using the Marshall mix design procedure. Four of the five Superpave sections had the same aggregate gradation, aggregate source and binder content, but different binder grades. The fifth Superpave section contained 15% RAP, but had the same virgin aggregate sources as the other Superpave sections. The virgin binder grade used in this RAP section was identical to the one used in Section 2, which was the control Superpave section. Table 1.1 shows test section details, and the layout of the test sections is reproduced here in Figure 1.1. All coring was done in the "Coring Regions" so that the majority of the test section could be preserved and its performance could be observed. Transition Regions between the test sections allowed the contractor to change from one mix to another.

Other details of the mix design, volumetrics and other test section information may be obtained from the SPR-2148 report (*2*). As a part of that earlier study, tests were conducted on binders recovered from the surface courses obtained at different ages. In addition, creep compliance and strength tests were conducted on plant-produced lab-compacted mixes. It was observed that the results of low-temperature tests on binders recovered from the surface cores corresponded well with the observed pavement distress. However, the results obtained from creep compliance and strength tests conducted on plant-produced lab-compacted mixes did not agree well with observed thermal cracking in the field.

To investigate this discrepancy, further long-term monitoring and testing of these test sections was proposed by the researchers and approved by the Study Advisory Committee. To attain these objectives, field cores were obtained from the test sections at the end of 9.5 and 12 years from the time of construction.

TABLE 1.1
Test Section Details

			P_b, %		V_a, %		VMA, %	
Section ID	**Binder Grade**	**Mix Design**	**JMF**	**QC**	**JMF**	**QC**	**JMF**	**QC**
S1	AC-20 (PG64-22)	M	6.2	5.5	4.0	7.6	16.5	14.8
S2	PG64-28	S	6.5	6.8	4.0	3.0	15.0	14.4
S3	PG58-28	S	6.5	6.8	4.0	4.3	15.0	13.9
S4	PG64-28 w/RAP	S	6.4	6.3	4.0	4.4	15.4	13.5
S5	PG70-28	S	6.5	6.2	4.0	5.1	15.0	15.0
S6	PG64-16	S	6.5	6.6	4.0	5.5	15.0	14.5

M = Marshall; S = Superpave

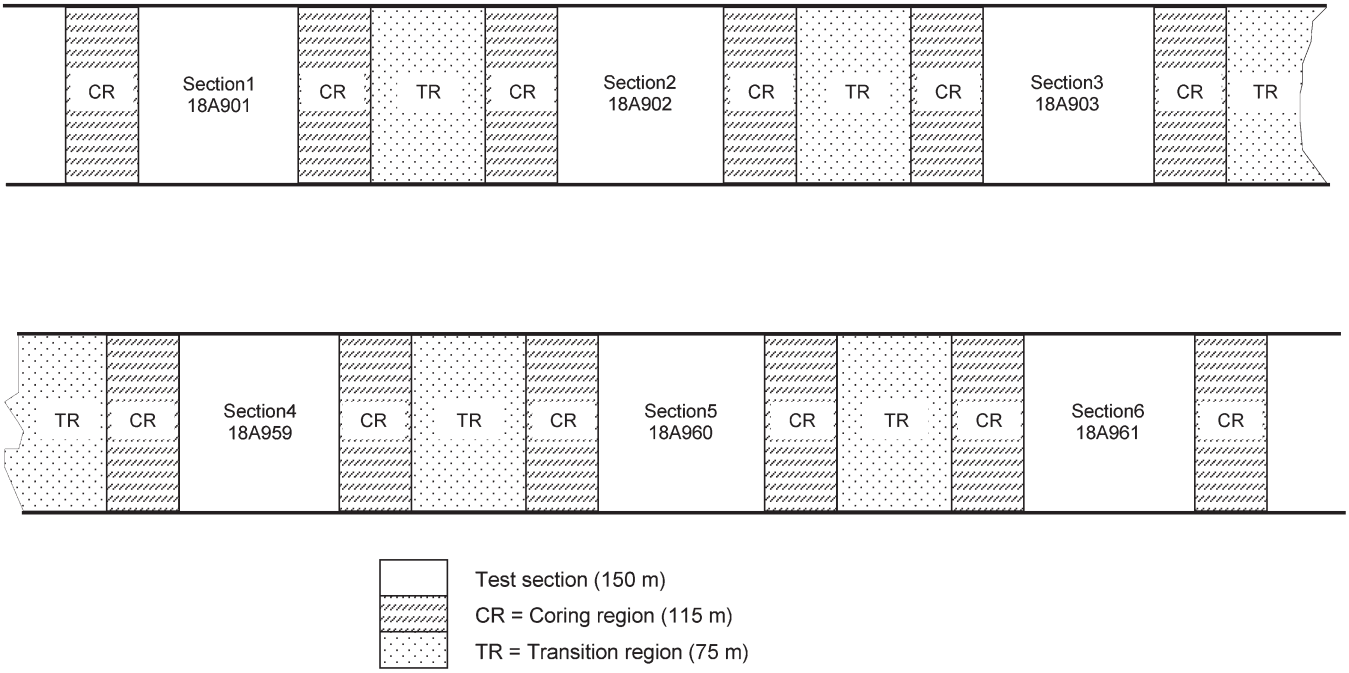

Figure 1.1 Layout of SPS9-A test sections.

Sufficient samples were collected to conduct creep compliance tests on the field cores, in addition to obtaining recovered binder. Results of the tests conducted on recovered binders and these two sets of field cores are presented in this report.

2. FIELD CORE VOLUMETRICS

This chapter describes the planned testing conducted on the obtained samples. The test results are described further in later chapters and summarized in the appendix. Supplementary data on the field performance monitoring from the LTPP Regional Contractor is also included in this report in Chapter 5.

2.1 Layer Thickness

Coring was conducted by INDOT Greenfield District personnel, and the cores were delivered to the North Central Superpave Center (NCSC) for testing. The surface and intermediate layers of the cores were first separated by sawing. The thickness of the surface layer and that of the first lift of the intermediate layer were also determined. The average thickness of the surface layer was in the range of 42–45 mm and 40–45 mm at the end of 9.5 and 12 years, respectively. The time, t, at which cores were taken is identified as G for t = 9.5 years and H for t = 12 years, according to the convention established by LTPP. The mean thickness and coefficient of variation of the ten core samples obtained from each section are presented in Table 2.1. No statistical differences in mean surface layer thickness were found between test sections at both ages. Similarly, the change in mean layer thickness of the surface layers between the two ages was not statistically significant. However, when compared with data from the initial set of cores obtained two weeks after construction, only Sections 1 and 6 showed no significant differences. Figure 2.1 shows trends in layer thickness during the lifetime of the test sections to-date. Overall, there is a slight decrease in layer thickness since the last set of cores collected prior to this study (at the end of four years). This may be expected due to wearing off of the surface layer with exposure to traffic over time and potentially consolidation under traffic. There is also, of course, construction variability in the depth of the compacted layers.

2.2 Bulk Specific Gravity (G_{mb})

Following the determination of the surface layer thickness, the in-place bulk specific gravity of the mixture was determined according to AASHTO T199. This test was also performed on the top lift of the intermediate layer samples. The results are presented in Tables 2.2 and 2.3, respectively. Figure 2.2 shows a leveling off in the bulk specific gravity of the surface layers in all sections after 4 years, except for Section 4 (with 15% RAP) which showed a slight increase (about 1.4%). Data from the intermediate layer cores (shown in Figure 2.3) showed a slight increase in the bulk specific gravity of all the test sections (0.5% to 1.5%). An increase in the bulk specific gravity translates to a decrease in percent air voids due to additional compaction with traffic, as will be presented later in this chapter.

Figures 2.2 and 2.3 also demonstrate that the bulk specific gravities increased in the surface and top lift of

TABLE 2.1
Thickness of Surface Layer

Section ID	Binder Grade	t = G (9.5 yrs.)		t = H (12 yrs.)	
		Mean (mm)	C. V., %	Mean (mm)	C. V., %
S1	AC-20	45	10.3	43	13.3
S2	PG64-28	43	4.6	44	8.2
S3	PG58-28	42	5.7	41	8.2
S4	PG64-28 w/RAP	42	9.1	41	9.3
S5	PG70-28	43	8.6	40	10.0
S6	PG64-16	43	9.3	41	9.8

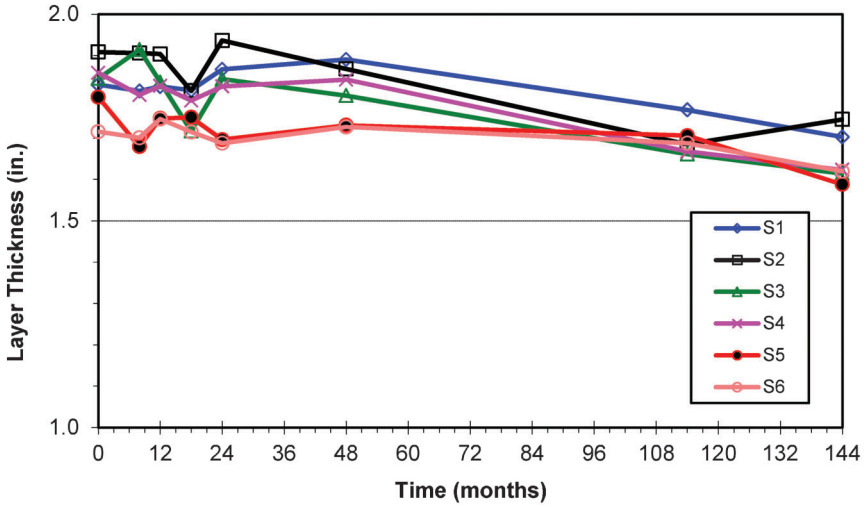

Figure 2.1 Trends in surface layer thickness.

TABLE 2.2
Bulk Specific Gravity of Surface Layer Cores

Section ID	Binder Grade	t = G (9.5 yrs.)		t = H (12 yrs.)	
		Mean	C. V., %	Mean	C. V., %
S1	AC-20	2.311	0.5	2.312	0.5
S2	PG64-28	2.402	0.3	2.391	0.5
S3	PG58-28	2.389	0.7	2.385	1.2
S4	PG64-28 w/RAP	2.360	0.6	2.374	0.7
S5	PG70-28	2.325	0.7	2.314	0.8
S6	PG64-16	2.316	0.7	2.320	0.4

TABLE 2.3
Bulk Specific Gravity of Intermediate Layer Cores (Upper Lift Only)

Section ID	Binder Grade	t = G (9.5 yrs.)		t = H (12 yrs.)	
		Mean	C. V., %	Mean	C. V., %
S1	AC-20	2.417	0.9	2.427	1.0
S2	PG64-28	2.402	0.8	2.419	0.5
S3	PG58-28	2.417	0.8	2.422	0.8
S4	PG64-28 w/RAP	2.419	0.8	2.423	0.8
S5	PG70-28	2.372	0.3	2.354	1.7
S6	PG64-16	2.353	0.4	2.355	0.5

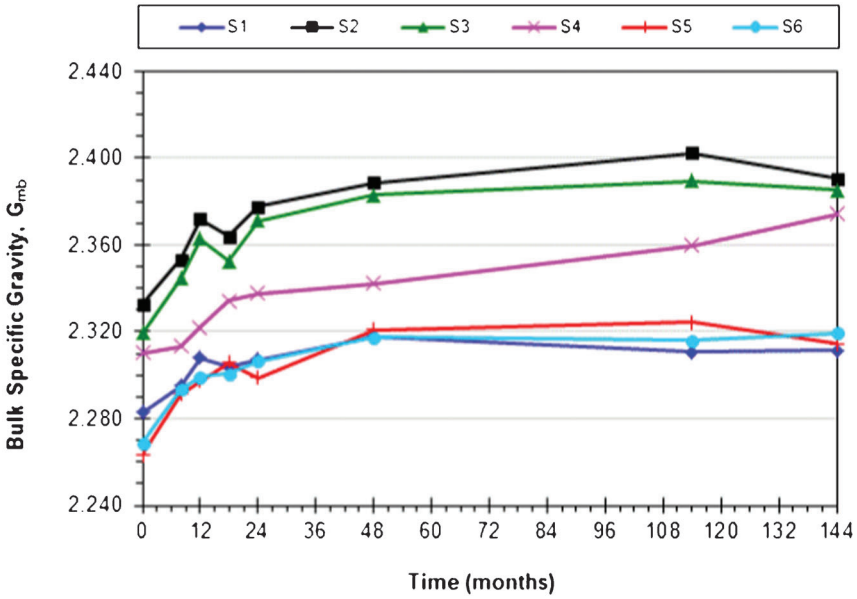

Figure 2.2 Trend in bulk specific gravity of the surface layer with age.

the intermediate course in all sections over the first two years in service. Details are provided in the SPR-2148 report (*2*).

2.3 Percent Air Voids and Other Volumetrics

The mixture volumetrics of the surface lifts were determined for the field cores at 9.5 and 12 years after construction. This data was combined with the information from the previous study to present the changes in volumetrics over the service life to date. The maximum specific gravity of the mixes (G_{mm}) was used along with the bulk specific gravities discussed in section 2.2 to determine the air void content. In addition, the binder content (P_b, %) was determined and used to calculate the voids in mineral aggregate (VMA) and voids filled with asphalt (VFA).

Figures 2.4, 2.5, 2.6 and 2.7 show the trends in P_b, V_a, VMA and VFA, respectively, in the surface mixes. No clear cut trend was observed in the asphalt content, except that the Marshall-designed mixture in Section 1 had a consistently lower binder content than the Superpave mixtures. All sections showed approximately 0.5% increase in the recovered binder content at the end of 9.5 years, followed by a drop at the end of 12 years, with the exception of Section 2 where it continued to increase. In all cases, there was an increase in the binder content of cores obtained at the end of 9.5 years in

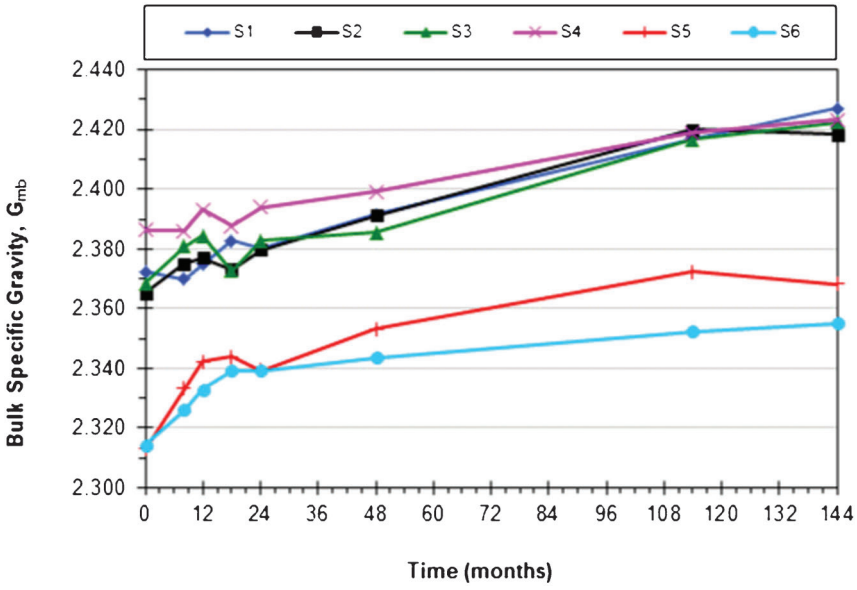

Figure 2.3 Trend in bulk specific gravity of the intermediate layer with age.

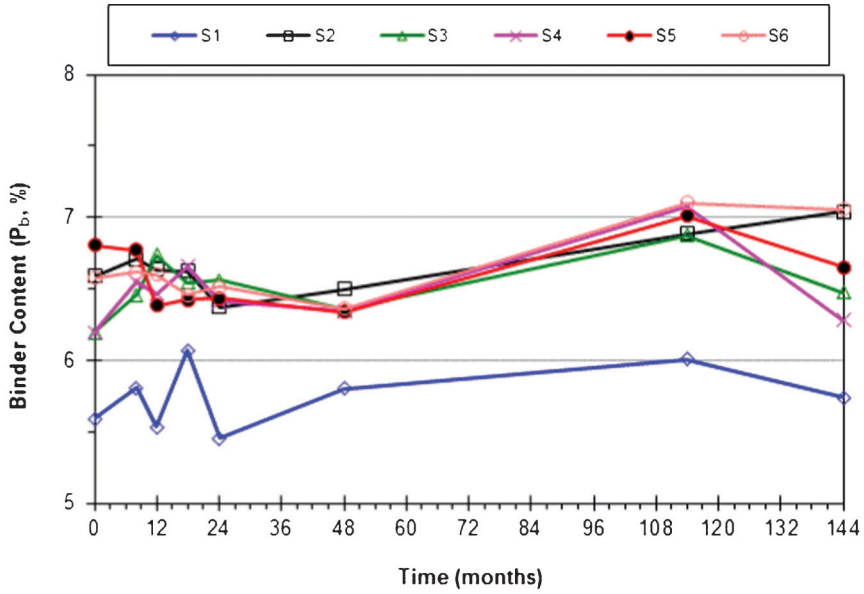

Figure 2.4 Trend in binder content of the surface layer.

comparison with the P_b at the end of four years. This was followed by a decrease in P_b by the end of 12 years, except for Section 2 which showed a slight increase. The reason for this variation in binder content is not known.

Due to the leveling off or slight increase of the G_{sb} after four years, either no significant change or a decrease in the percent air voids (V_a, %) would be expected in the field core samples. This is reflected in Figure 2.5, where most of the sections show a decrease in percent air voids from that observed at the end of the earlier study (four years), except Section 4. This decrease is expected due to densification under traffic and clogging of the voids on pavement surface with dust and other fine particles due to the natural attrition occurring in-service. The air void content of Section 2 fell below 2% by the 9.5-year mark. An air void content of less than 2% is often related to excessive mix plasticity which could be exhibited in the form of shoving.

The VMA, shown in Figure 2.6 appears to have either leveled off or shows slight change after four years. With the exception of Sections 4 and 6, the VMA of the remaining sections fell below the AASHTO MP2-95 (now AASHTO M323) recommended minimum value of 15%. The changes in VMA and V_a are reflected in the VFA of the mixes, shown in Figure 2.7. Per AASHTO MP2-95, it is desirable for VFA to be between 73–76% at time of construction. At the end of 12 years in service, none of the test sections satisfied this

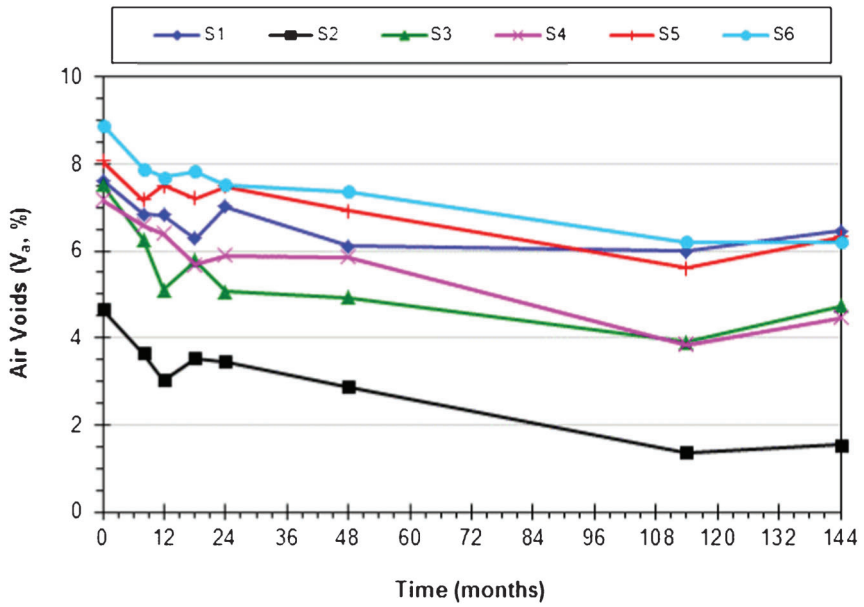

Figure 2.5 Trend in air content of the surface layer.

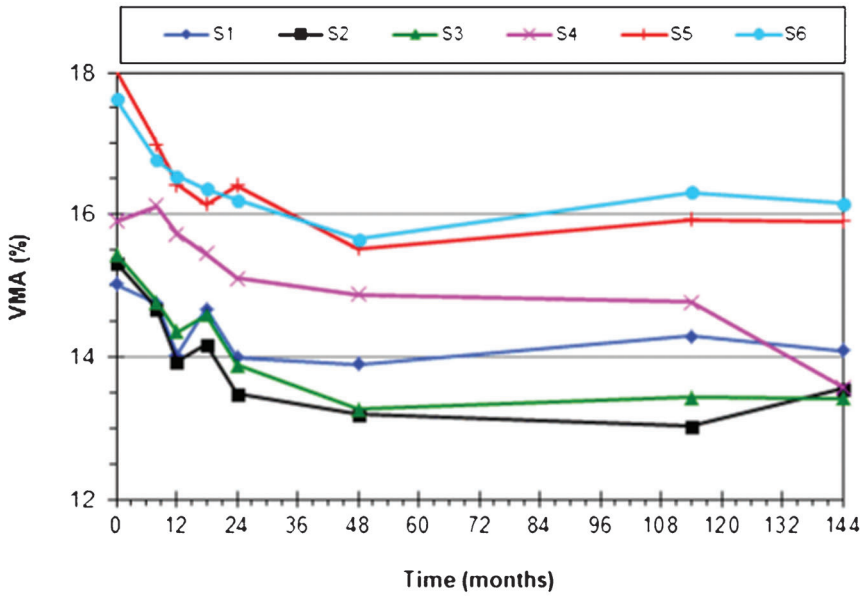

Figure 2.6 Trend in VMA of the surface layer.

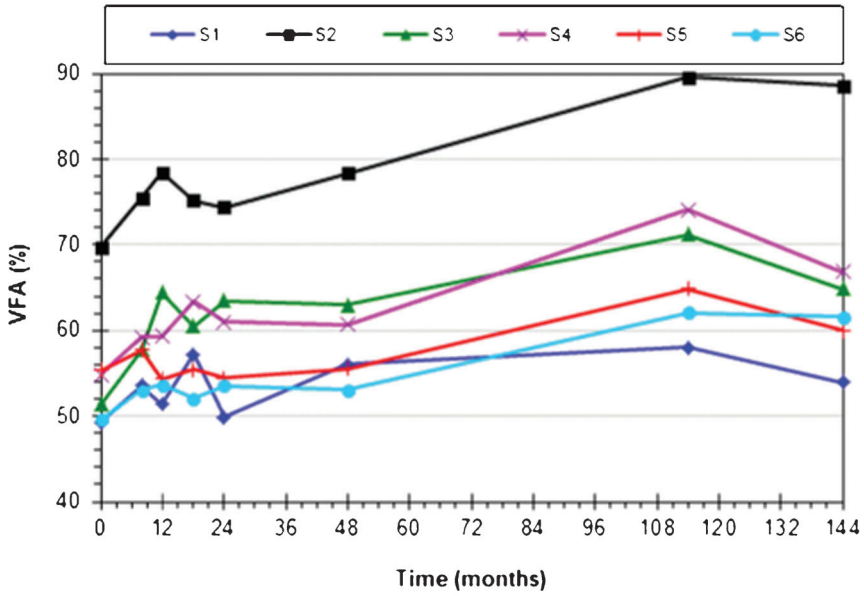

Figure 2.7 Trend in VFA of the surface layer.

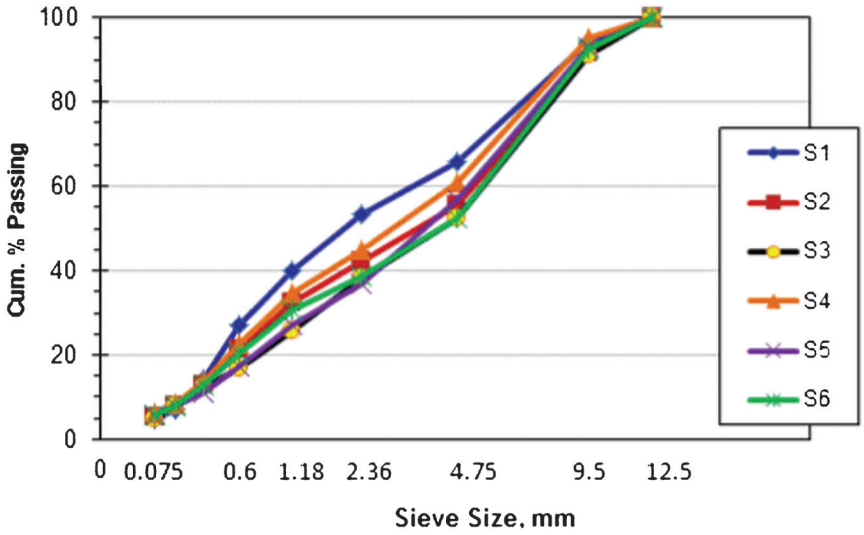

Figure 2.8 Gradations of test sections at the end of 12 years.

requirement. However, these mixture volumetric requirements are critical only during the initial pavement construction phase, and are only mentioned here to serve as a reference.

2.4 Gradation

After the binder extraction process, mechanical analysis of extracted aggregate was conducted to determine the particle size distribution of the aggregate in the surface mixes, according to AASHTO T30. Figures A.1 through A.6 in the appendix show the gradation plots for the six test sections at different ages. As these graphs indicate, all the plots from the different ages overlapped and formed a narrow band, indicating that there was no significant degradation of aggregate over time and that the mix placement was uniform (no segregation).

Figure 2.8 shows the particle size analysis conducted on extracted aggregate obtained from the last set of surface layer cores (age = 12 years). Mixes from Sections 2, 3, 5 and 6 had the same JMF gradation, while Section 4 (with 15% RAP) and Section 1 with Marshall design had different gradations. This is clearly reflected in Figure 2.8 where Sections 2, 3, 5 and 6 appear closer together, while Sections 1 and 4 are set apart from this cluster.

3. BINDER TEST RESULTS

Two sets of core samples (6-in. dia.) were collected from the test sections at the end of 9.5 and 12 years, respectively. Each set consisted of ten cores from each test section. The surface layer of each core was separated from the underlying material and set aside for mixture and binder testing. Of the ten cores obtained from each section, seven were used for extraction and recovery of the binder and the remaining three were used for creep compliance and strength testing at low temperatures using the Indirect Tensile Tester (IDT), discussed later in Chapter 4. Binder extraction was done using the centrifuge method (AASHTO T164-97 Method A) with an 85% ethanol + 15% toluene blend as solvent. Following the extraction process, binder was recovered using the Rotavapor apparatus (ASTM D5404-93) and stored in sealed containers for testing.

Tests conducted on the recovered binder included penetration, specific gravity, shear modulus using the Dynamic Shear Rheometer (DSR), flexural stiffness using the Bending Beam Rheometer (BBR), and failure stress and strain at low temperatures using the Direct Tension Tester (DTT). These data will be summarized in the following sections.

3.1 Specific Gravity and Penetration

The specific gravity of a material is a measure of its density at a specific test temperature, which in turn influences its viscosity. This test was performed on the recovered binder in accordance with AASHTO T228-96 at 16°C. The average of two replicates was taken and is presented in Figure 3.1 as data points at 114 and 144 months, representing 9.5 and 12 years, respectively. During the early age of the pavement (up to four years), an increase in specific gravity was observed which may be attributed largely to age hardening of the binders. Incorporation of microscopic dust particles during the recovery process may also contribute to the apparent hardening to some extent. Beyond four years, no significant change was observed in the recovered binders from four of the test sections. Binders recovered from Sections 2 and 5 appeared to show a slight decrease (2.5 and 1.8%, respectively) beyond four years. No explanation for this behavior could be found, and repeat testing was performed to verify the data. While

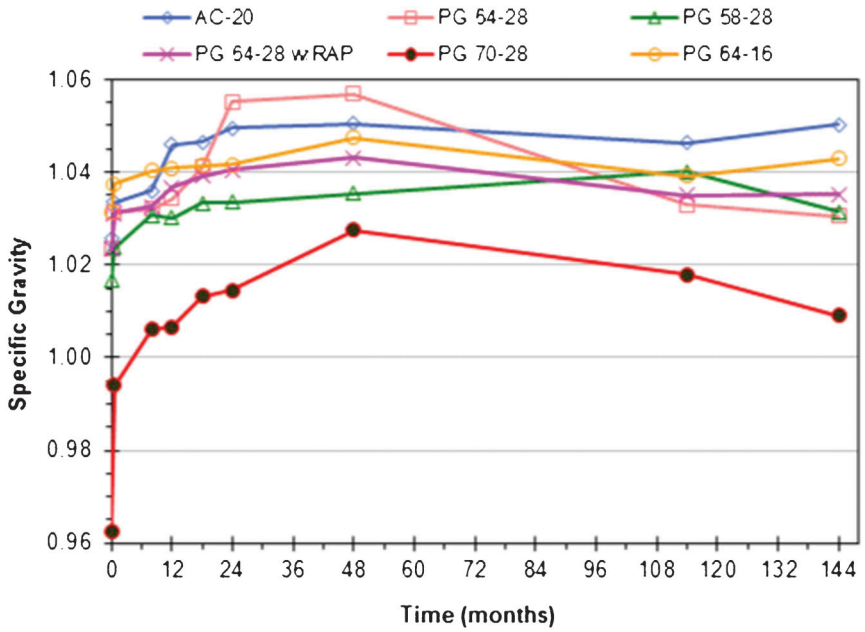

Figure 3.1 Change in specific gravity of recovered asphalt with age.

this may be attributed to leftover solvent in the binder during the recovery process, this supposition was not supported by other binder test data. Table A.3 in the appendix shows the data points plotted in this graph.

The penetration test was conducted at 25°C and 5°C according to AASHTO T49-89, and the data is presented in Figure 3.2 and Figure 3.3, respectively. No further hardening of the asphalt was observed, using this test method, after the second or fourth year after placement.

3.2 Complex Shear Modulus

The complex shear modulus of the recovered binders from the surface layer was determined at different temperatures and frequencies (i.e., frequency sweep at 6°-increments from 46°C to 76°C). The RTFO parameter, $|G^*|/\sin\delta = 2.2$ kPa, was used to determine the critical passing point at high temperatures (T_{DSR}). With time, as the pavement ages due to exposure to environmental and traffic conditions, the binder

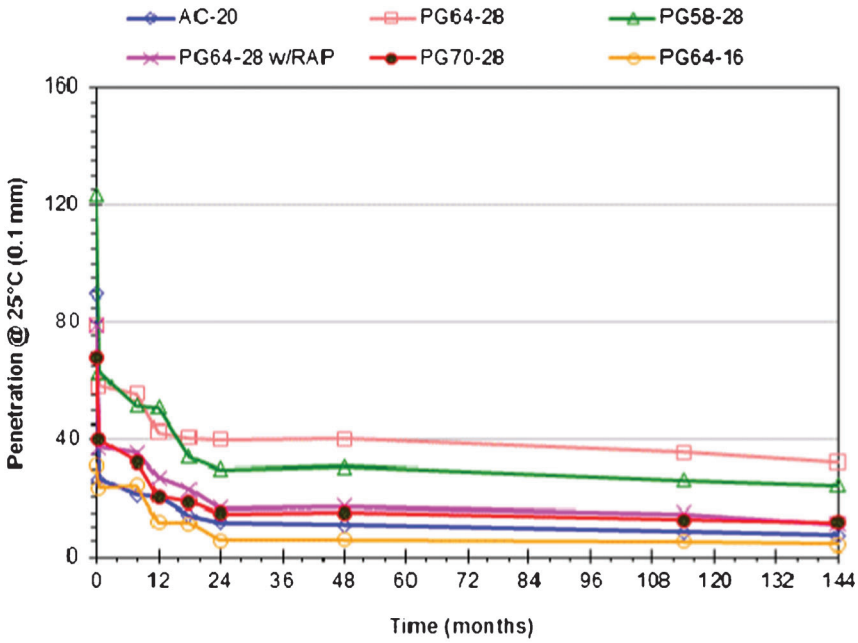

Figure 3.2 Change in penetration of recovered asphalt with age (25°C).

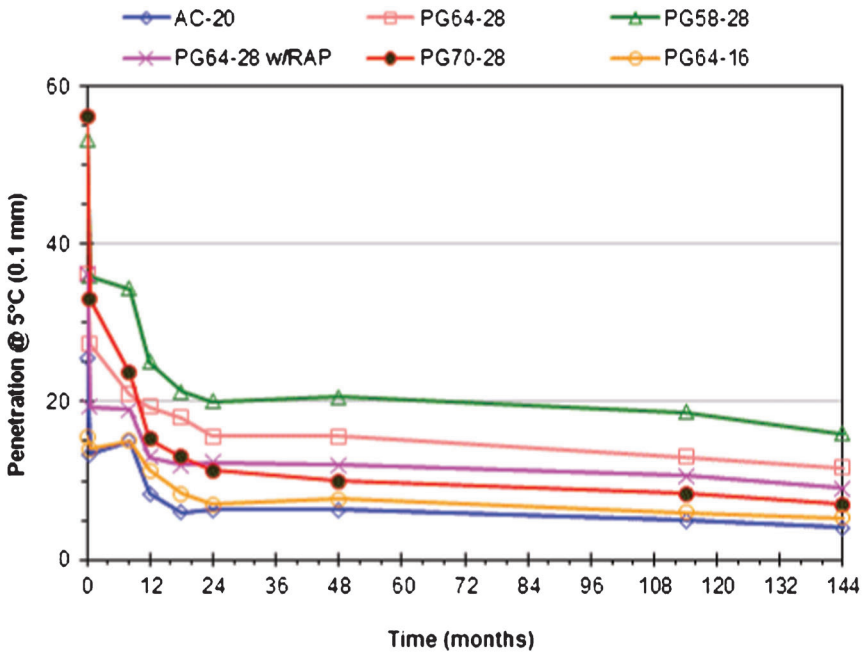

Figure 3.3 Change in penetration of recovered asphalt with age (5°C).

recovered from the surface layer is expected to show stiffening which is reflected as an increase in the critical passing temperature or the shear modulus at a given temperature.

A Bohlin CVO-II dynamic shear rheometer was used to perform these tests. Two replicates of each sample were tested and the average is presented in the graph shown in Figure 3.4. Except for binder recovered from Section 5 (PG70-28), all the remaining binders showed an increase in T_{DSR}, indicating a stiffening effect with the age of the pavement. The similar slopes of the trend lines indicate similar rates of aging. It can also be observed that at the end of 12 years, the high-temperature binder grade was increased by one level (6-degree increment) with respect to the original, tank binder used. The binder recovered from Section 4 with PG64-28 and RAP was consistently stiffer than the PG64-28 binder from Section 2 without RAP. Even in the case of binder from Section 5 that showed minimal aging, there was an increase in T_{DSR} with respect to the tank binder. If the tank binder data point for PG70-28 were to be omitted as an outlier, the R-squared value would increase to 73%. The binder used in Section 3 was of a softer grade and this is reflected in its lower stiffness all through the study period. Similarly, the stiffer binder used in Section 5 stayed consistently higher than the other binders in the study, during the whole study period.

As mentioned earlier in this report, the last set of field cores obtained for the previous study was at the end of four years, while the current study cores were obtained at the end of 9.5 and 12 years (t = G and H,

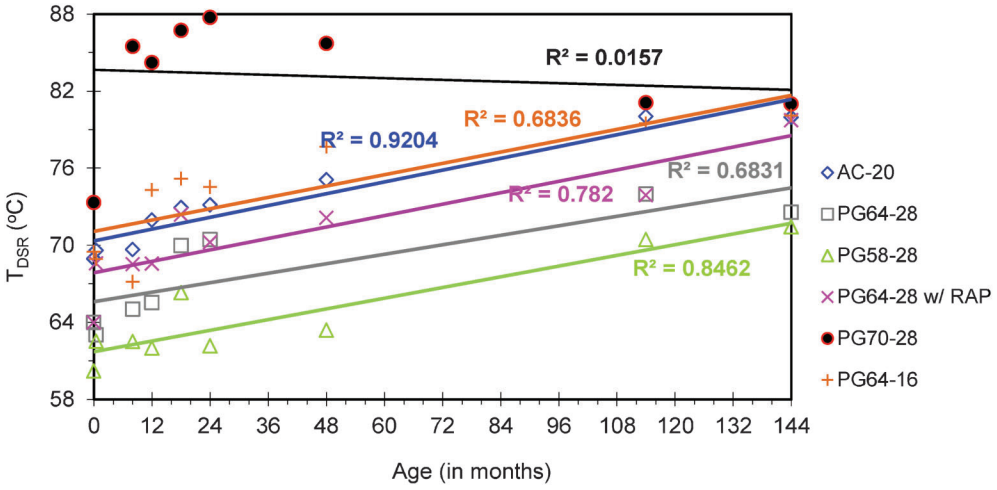

Figure 3.4 Change in T_{DSR} of recovered binders with time.

respectively). Based on the observed trends, it can be seen that in situ aging of the binder continued beyond the initial four years until the end of this study period (12 years since construction). Although the changes between the 9.5- and 12-year data points do not appear to be visually significant, excluding the last data point did not improve the R-squared value of the trend lines.

The solvent used for the centrifuge extraction process (AASHTO T164 Method A) was a blend of 85% toluene and 15% ethanol, followed by binder recovery using a Buchï® Rotavapor (ASTM D5404). Care was taken to minimize prolonged exposure to heat while ensuring that all the solvent was removed during recovery of the asphalt binder. Additionally, inline filters were used during the recovery process to remove any fines that were not removed by the fines centrifuge.

Applying time-temperature superposition, the frequency sweep data were used to create master curves for the binders tested in this phase of the study. Binders from the earlier study were retained in sealed containers kept at room temperature. The frequency sweep was also performed on these binders and master curves were generated. Data from the first set of field cores (2 weeks old, t = A) and binders recovered at the end of previous study (4 years old, t = F) were plotted for comparison along with the current set (t = G and H) for each test section. Only the master curves for Section 1 binder, AC-20, are shown here as an example in Figure 3.5, while the complete set is included in the appendix (Figures A.7 through A.12). For Section 5, binder recovered from 8-month old cores (t = B) is shown instead due to lack of binder from the two week old cores (t = A). The increase in stiffness of the recovered binders with increasing age is reflected in all the test sections. The plots tend to converge at low temperature (high stiffness) and diverge at high temperature (low stiffness).

3.3 Creep Stiffness and Slope

To determine the low-temperature passing grade of the binders, a Cannon® Bending Beam Rheometer was used to measure the creep stiffness and slope, following AASHTO T313. The recovered binders were not aged further after the extraction process, to capture the properties of the recovered binder at the given age of the cores. The warmer of the two temperatures obtained from m-value of 0.300 and stiffness of 300 MPa was used as the controlling critical temperature (T_{BBR}) from this test procedure. These data are presented in Figure 3.6 as a function of the age of the recovered binder.

The flatness of the lines for the PG58-28 and PG64-28 binders indicates that there was no perceptible increase in the low-temperature stiffness of these binders during the 12 years of the study period. A stronger linear trend was observed in the case of binders recovered from Section 1 (AC-20), Section 4 (PG64-28 w/RAP) and Section 5 (PG70-28). In particular, data from Section 5 showed the highest R-squared value and the steepest slope, indicating that this binder underwent the highest degree of aging (stiffening) as determined by the BBR at low temperatures. This is contrary to the trend observed at high temperatures where the shear modulus was measured using the DSR at high temperatures. In that case, Section 5 binder did not show any stiffening with age, whereas all the other binders showed similar stiffening behavior, as evidenced by their slopes in Figure 3.4.

3.4 Thermal Stress Analysis Routine (TSAR®)

The critical cracking temperature can also be determined using a software package called TSAR® developed by Abatech, Inc. (*3*). Using compliance data

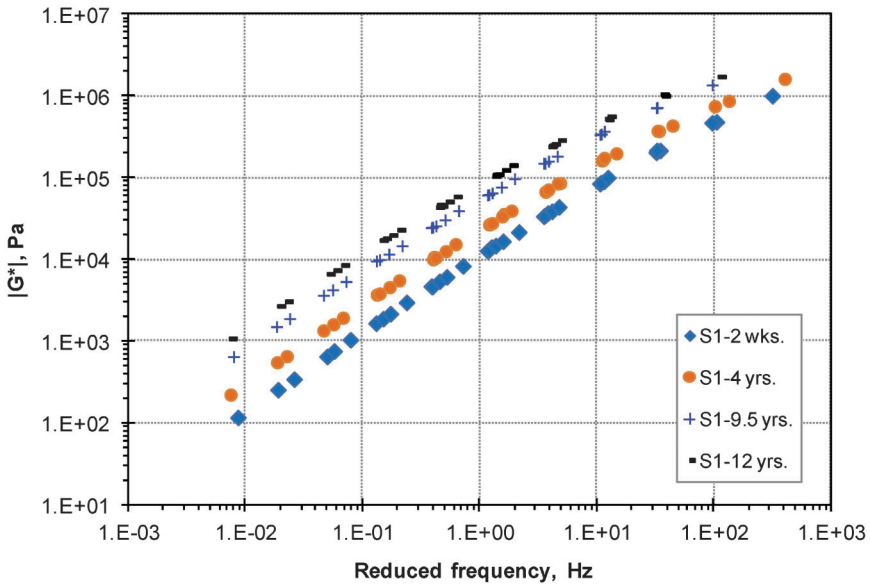

Figure 3.5 Master curves for AC-20 recovered from Section 1.

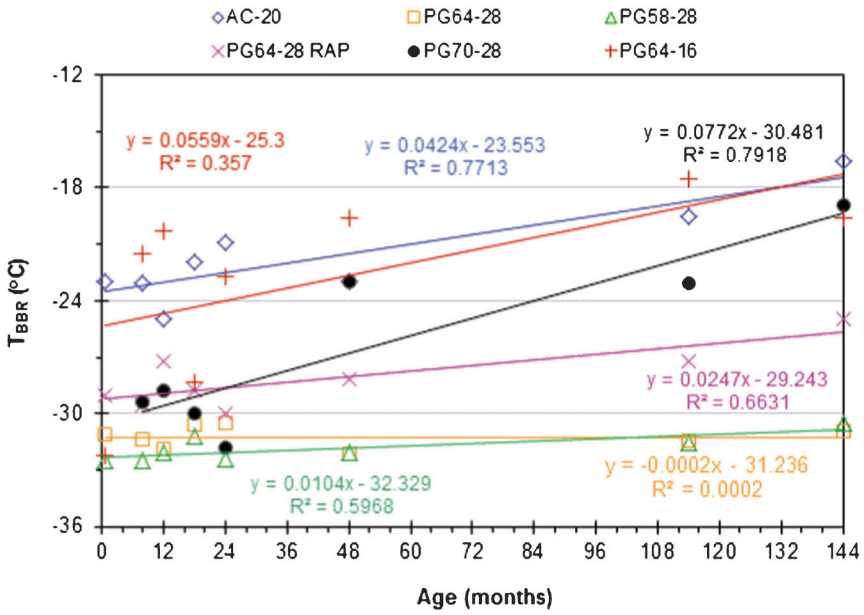

Figure 3.6 Trend in T_{BBR} as a function of age of the pavement.

from the BBR, the Christensen-Anderson-Marasteanu (CAM) model (*4*) is applied in creating the master curves for the recovered binders using this software. Tensile stress data from an Instron® Direct Tension Tester were used to determine the failure stress and strain of the recovered binders at low temperatures, according to AASHTO T314. The intersection of the thermal stress and strength lines yields the critical cracking temperature (T_{TSAR}), as this reflects when the stresses building up in the binder as the temperature decreases eventually exceed the strength of the binder.

Data from the previous study cores (A = 2 wk. and F = 4 yr.) are superimposed along with data from the current study cores (G = 9.5 yr. and H = 12 yr.) for comparison and are presented in Figure 3.7. The plots for the remaining test section binders are shown in the appendix (Figures A.13 through A.18). In general, a stiffening in the thermal stress with increasing age of the recovered binder can be seen in all the test sections. It is generally observed that stiffer pavements fail by thermal cracking at warmer temperatures than softer mixes. The most significant change was observed in the case of Section 6, while Sections 3 and 4 showed the least change as evidenced by the clustering of the thermal stress curves. No defining trends were observed in failure strength of the recovered binders with age.

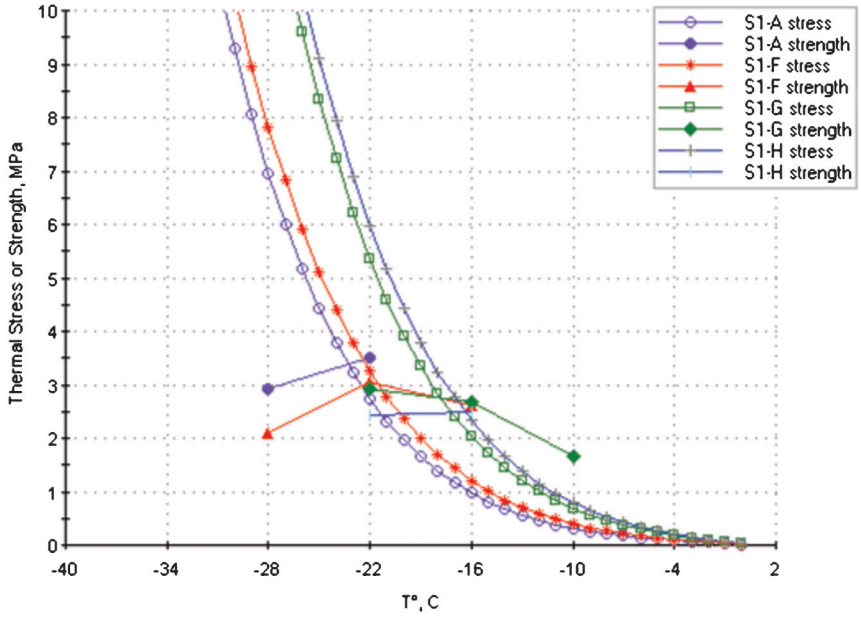

Figure 3.7 Thermal stresses in the pavement—Section 1.

TABLE 3.1
Critical Pavement Temperature Obtained from Recovered Binder Tests

Section ID	Binder Grade	t = G (9.5 yrs.)		t = H (12 yrs.)	
		T_{BBR}	T_{TSAR}	T_{BBR}	T_{TSAR}
S1	AC-20 (PG64-22)	−19.8	−17.8	−16.6	−16.4
S2	PG64-28	−31.5	−31.8	−30.9	−29.2
S3	PG58-28	−31.5	−27.5	−30.5	−29.3
S4	PG64-28 w/RAP	−27.3	−26.2	−24.9	−24.9
S5	PG70-28	−21.1	−30.3	−19.1	−24.9
S6	PG64-16	−17.5	−18.0	−19.3	−19.5

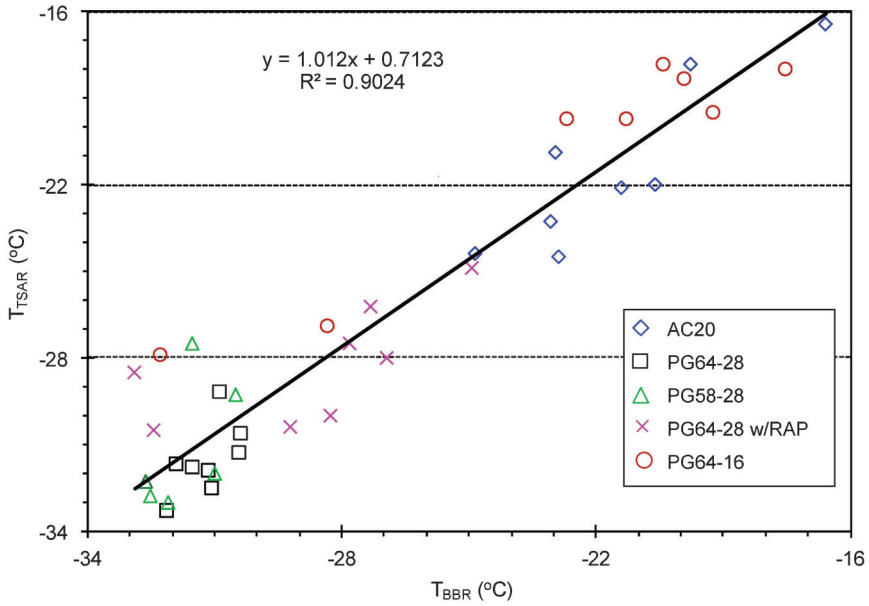

Figure 3.8 Comparison of T_{BBR} versus T_{TSAR}, excluding PG70-28 data.

Table 3.1 shows the critical temperature obtained from TSAR and BBR data from recovered binders at the end of 9.5 (G) and 12 (H) years. Neglecting the modified binder (PG70-28), good similarity can be observed between the two sets of data points. The critical temperature for binder recovered from the RAP section (S4) was warmer than that of the control section (S2) without RAP. This is indicative of binder stiffening and may be attributed to the contribution of the binder recovered from the RAP present in the mix. Sections 2 and 3 with the same low-temperature grade (PGxx-28, unmodified) had similar cracking temperatures. Recovered binder test data from these field cores indicate that they still satisfy the PG requirement at low temperature, for Sections 1, 2, 3 and 6, implying that thermal cracking may be expected only in Sections 4 and 5 at the end of 12 years.

Finally, a comparison of critical temperatures from the BBR testing and DT testing (T_{BBR} versus T_{TSAR}) from all ages showed good correlation between the two methods (R-squared = 77%). When the data points from PG70-28 (modified binder) were removed, the R-squared value increased to 90%. This plot is shown in Figure 3.8. It can be seen from the plot that the critical temperature for binders with a warmer low-temperature grade, i.e., PG64-16 and AC-20 (PG64-22), tended to fall towards the upper right corner (warmer) as expected. Binders with PGxx-28 tended to cluster at the lower left corner (colder) of the graph.

4. LOW-TEMPERATURE TESTING OF FIELD CORES

Three of the core samples obtained from each test section of the pavement at the end of 9.5 and 12 years were retained for low-temperature testing, while the remaining were used for binder extraction and recovery as mentioned in Chapter 3. Creep compliance testing of the surface and intermediate course samples was conducted at -20, -10 and 0°C, followed by strength testing in accordance with AASHTO T322, using the Instron® Indirect Tensile Tester. The Excel program LTSTRESS, used to determine thermal stresses in the pavement as a function of temperature, was developed by Don Christensen based on the procedure described by Roque and Hiltunen (5) and modified by

Christensen (*6*). The cores' average air voids, strength and mixture stiffness at 60 seconds are presented in Tables A.6 and A.7 of the appendix. Graphical representations of the creep stiffness and temperature data for the surface and intermediate layers are shown in Figure 4.1 and Figure 4.2, respectively.

In the surface and the intermediate layers, the stiffness and cracking temperature exhibit a parallel trend, i.e., as the stiffness drops (mix becomes more flexible) the temperature also drops (cracks at a colder temperature). This agrees well with the expected behavior of HMA mixtures at low temperatures, where the stiffer mixes fail at warmer temperature and vice versa.

Among the surface layer cores (Figure 4.1), Section 1 (Marshall design), with AC-20 binder that graded as a PG64-22 under the Superpave system, was the stiffest, while Superpave mixes S5 and S6, with PG70-28 and PG64-16, respectively, were the softest. The binder used in Section 3, PG58-28, was softer than the binder used in the control mix, Section 2, as expressed by the lower stiffness and correspondingly lower cracking temperature but the difference was less than one binder grade. The mix with 15% RAP (S4) was slightly stiffer than the control mix, with similar cracking temperature. The stiffness of the mix with the SBS-modified binder (S5) was lower than that of the control mix, but on par with that of the mix with the soft binder (S3) and that used in Section 6. There was one binder grade difference between the critical temperature of S2 and S5, despite the fact that both binders met the same low-temperature grade (-28). For mixes in which the critical cracking temperature of the surface layers was warmer than that indicated by the binder grade, severe cracking could be expected in the pavements in the field. Accordingly, these data obtained from IDT testing of field cores obtained at the end of 9.5 years indicate that all the test sections will exhibit thermal cracking.

Data from creep compliance testing of the cores from the intermediate layer are shown in Figure 4.2.

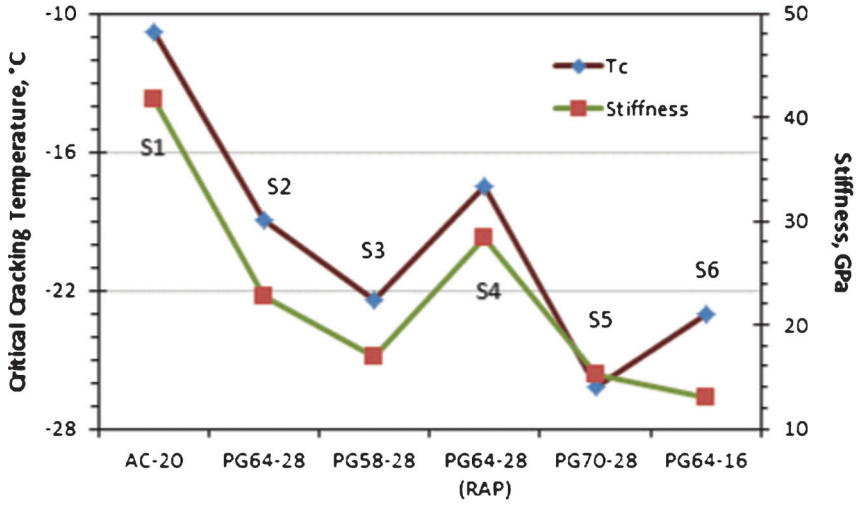

Figure 4.1 Cracking temperature and mixture stiffness of the surface layers.

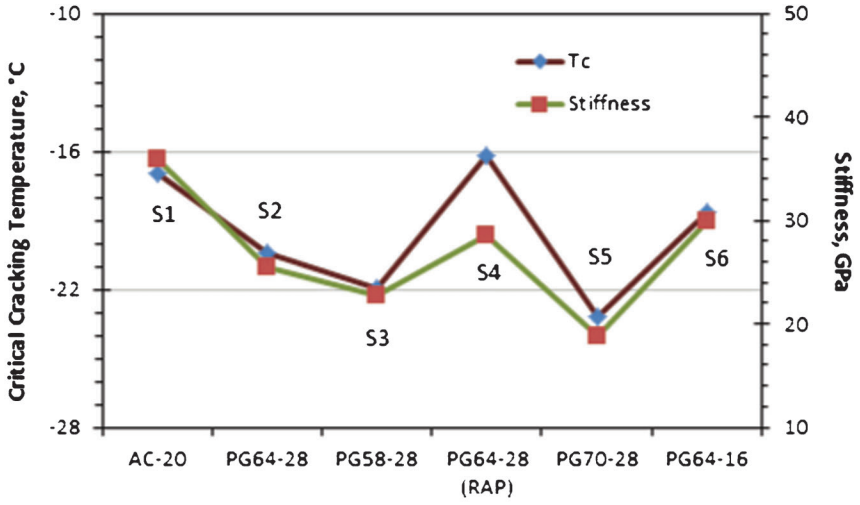

Figure 4.2 Cracking temperature and mixture stiffness of the intermediate layers.

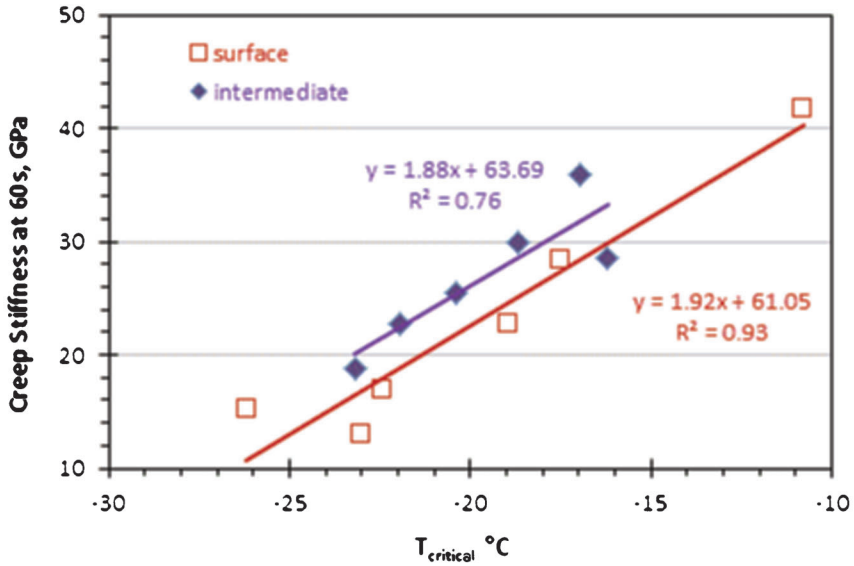

Figure 4.3 Relation between stiffness and critical cracking temperature.

As in the case of surface mixes, the stiffness and cracking temperature of the intermediate layer mixes also reflect a parallel trend. Once again, Section 1 exhibited the highest creep stiffness; the RAP mix was stiffer than the control mix, albeit only slightly; and Section 5 had the lowest stiffness. There was less spread in the T_c and stiffness data from the intermediate layer mixes when compared with the surface layer mixes and the differences in the cracking temperature between any two test sections never exceeded one binder grade.

To further emphasize the relationship between mixture stiffness at 60 s and the critical cracking temperature of the pavement (mix), a regression line between the two factors was fitted as illustrated in Figure 4.3. Both trend lines exhibited similar slopes, i.e., both mixes showed similar change in stiffness for a given change in temperature. The intermediate mixes have a smaller range in temperature and stiffness data compared to the surface mixes, suggesting a lesser variability in the stiffness and cracking temperature of the intermediate mixes specific to this study.

The development of thermal stresses in the pavement as the temperature falls below freezing is shown in Figures 4.4 and 4.5, for the surface and intermediate mixes, respectively. Typical failure strength of hot mix asphalt at low temperature is in the range of 300 - 500 psi. Examining the behavior of mixes below 4000 kPa (~600 psi), it is clearly evident from Figure 4.4 that mix from Section 1 was the stiffest among all the mixes and the mix used in Section 5 (with the SBS-modified binder) was the most flexible. Initially, Sections 2 and 4 (control vs. RAP section) showed similar stress development, but as the temperature fell below -10°C the lines diverged, with the

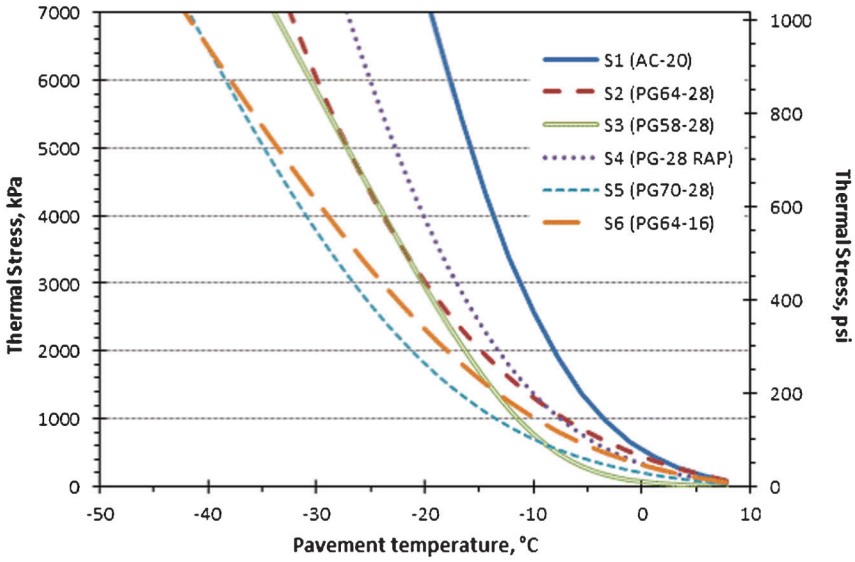

Figure 4.4 Thermal stress versus pavement temperature in the surface layer mixes.

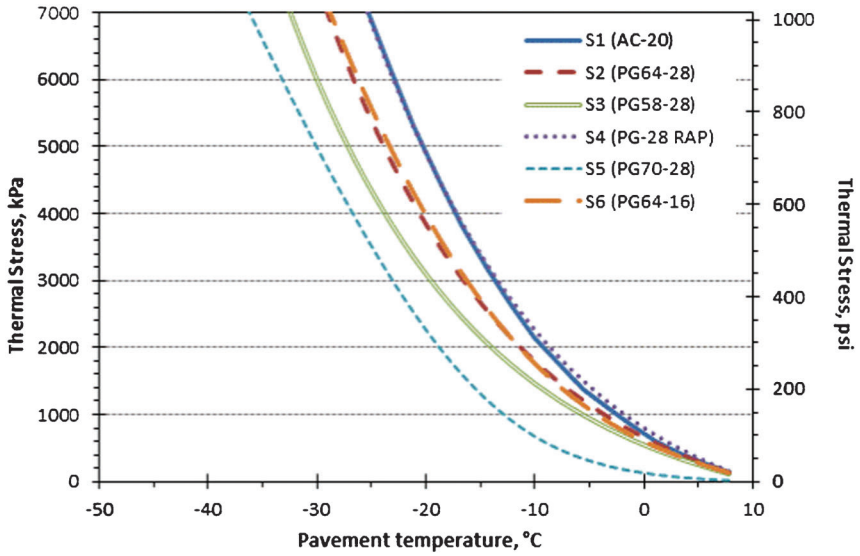

Figure 4.5 Thermal stress versus pavement temperature in the intermediate layer mixes.

RAP mix being stiffer than the control mix as anticipated. Section 3, with the softest binder, was initially less stiff than Section 5 as well, but as the temperature dropped below -10°C the effect of SBS-modification was expressed by the increased flexibility of the mix. In the case of intermediate course mixes, the Marshall mix (S1) and RAP mix (S4) showed almost identical stress development and were the stiffest of the six sections. The mixes used in the control section (S2) and Section 6 also showed similar stress gains. Once again, the Section 5 mix was the most flexible followed by the Section 3 mix with the soft binder.

5. FIELD DISTRESS SURVEY DATA

Manual and photographic distress surveys for this SPS site were conducted by the North Central Regional Coordinators, ERES Consultants, during the initial study period. Survey data included crack length and frequency of occurrence, longitudinal and transverse profiles, International Roughness Index (IRI), etc. Manual distress surveys of these test sections were conducted in July 1998 and February 2001, after 1 and 3.5 years in-service, respectively. Further details about the manual survey data may be obtained from the earlier report titled *Development of Indiana's SPS9-A Site* (*2*). Extensive patching was performed on some of the test sections by the local INDOT maintenance unit after the last survey in 2003, hence this SHRP site was classified as "out-of-study" by the LTPP program office in September 2004 and no further distress surveys were conducted after this rehabilitation (Figure 5.1 and Figure 5.2). The data presented below were made available through the LTPP database (*7*).

5.1 Photographic Surveys

Photographic surveys of the 150-m monitoring regions of each test section were conducted after three years (August 2000) and six years (July 2003) from the time the pavement was first put into service. This was done on 35-mm black and white film, typically covering a 4-m wide area and interpreted using PADIAS software version 4.2. Since the LTPP database does not distinguish between reflective cracking and those caused by excessive build-up of thermal stress (i.e., low-temperature cracking), the transverse crack data presented here may represent a combination of the two types of cracks. Figure 5.3 and Figure 5.4 show the trends in transverse and longitudinal cracking observed in the test sections, respectively. The relative number and length of low, medium and high intensity cracks are shown in Tables A.9 through A.11 of the appendix.

At the end of three years in service, no transverse cracking was observed in the sections with unmodified PGXX-28 binder (S2, S3 and S4 w/RAP). The section (S5) with modified binder, PG70-28, had already started to show transverse cracking at this age. The Marshall section (S1) with AC-20 (= PG64-22) experienced slightly lower crack intensity than the section with PG64-16 (S6). Similar trends were observed at the end of

Figure 5.1 Rehabilitation of the SPS9-A study site.

Figure 5.2 Punchout between Sections 5 and 6 (left) and subsequent patching (right).

six years, with S5 exhibiting the highest amount of cracking and S3, with the soft binder, showing minimal cracking. The RAP section (S4) also showed cracking, but to a lesser extent than that observed in sections with PG64-16 (S6) and PG64-22 (S1 with AC-20). The section with modified binder (S5, PG70-28) shows the greatest amount of transverse cracking, which is not expected.

While all the sections performed relatively well in withstanding low-temperature stresses at the end of three years, all sections showed longitudinal cracking outside the wheel path to various degrees. Trends similar to those observed in transverse cracking were also evident in longitudinal cracking, such as, S3 with the softest binder performed better than all the other sections, S4 showed more cracking than the control probably due to the presence of RAP, and S5 showed the highest amount of cracking comparable with S6, etc. At the end of six years, however, all sections showed similar amounts of cracking, with S5 still leading the ranking and S3 in the last position. A minimal amount of wheel path cracking ($<$ 2 m combined length), typically considered load-induced, was observed in all sections, except S5, which showed significant distress (65 m combined length).

5.2 Longitudinal Profile

Longitudinal profile measurements along the left and right wheel paths were conducted using the following inertial profilers; K. J. Law Engineering T6600 between 1997 and 2001 and International Cybernetics MDR4086L3 in 2003 and 2004. Moving averages were computed at 0.300-m intervals (0.98 ft) and profile data was stored at 0.150-m intervals. Five runs for each test section were routinely conducted at an average speed of 80 kph. Between August of 1997 and August of 2004, seven such profile measurements were conducted and stored in the LTPP database. Figure 5.5 shows the initial profile of Sections 1 and 2 taken soon after ($\sim$ 3 mo.) pavement construction was completed, and at the end of approximately seven years. The profiles of the remaining sections are shown in the appendix.

Section 6 and Section 3 show fairly uniform profiles in comparison with all the other sections. The change in elevation stayed within a narrow range of $\pm$ 5-in. range for these two sections. The control section (S2) and RAP section (S4) showed large changes, i.e., steep peaks and deep valleys, within the length of the 150-m monitoring region of the section. In all sections, it can be seen that the "peaks" or high points that were observed in the initial survey were leveled off due to compaction by vehicular traffic, while "valleys" or low points were filled in due to material being shoved in from neighboring regions. The operator of the profilometer noted that rutting was observed in both wheel paths of all the test sections at the time of the final survey.

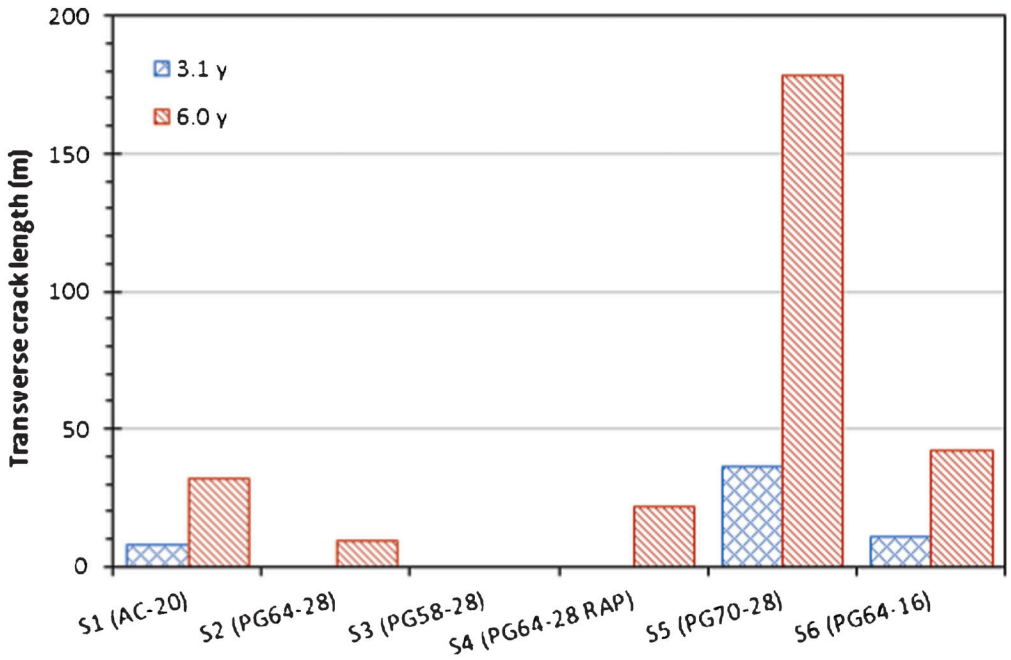

Figure 5.3 Transverse cracking from photographic surveys.

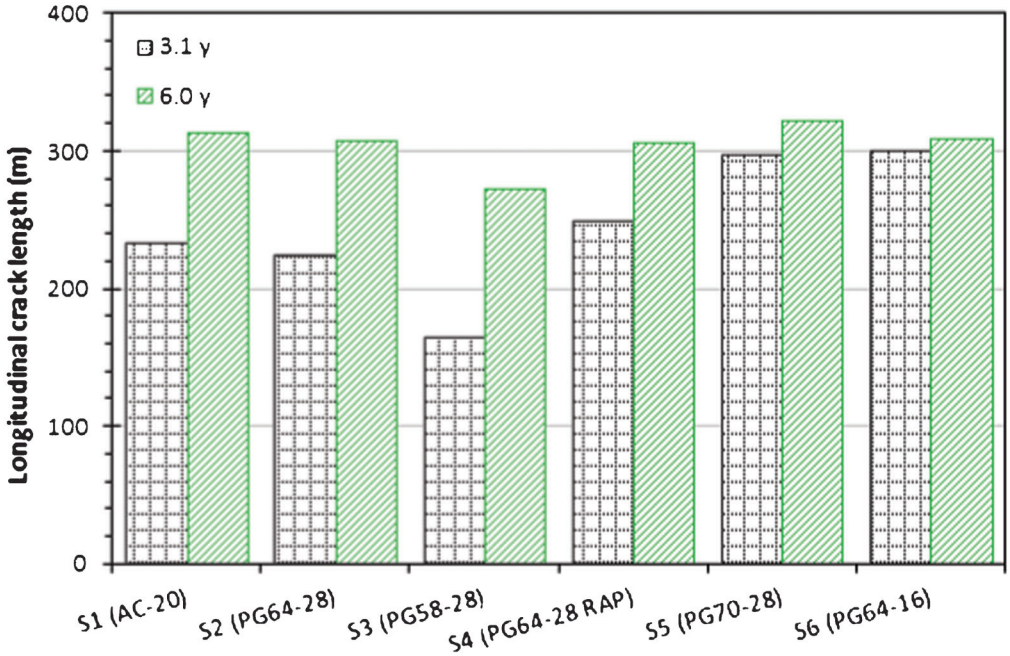

Figure 5.4 Longitudinal cracking outside the wheel path from photographic surveys.

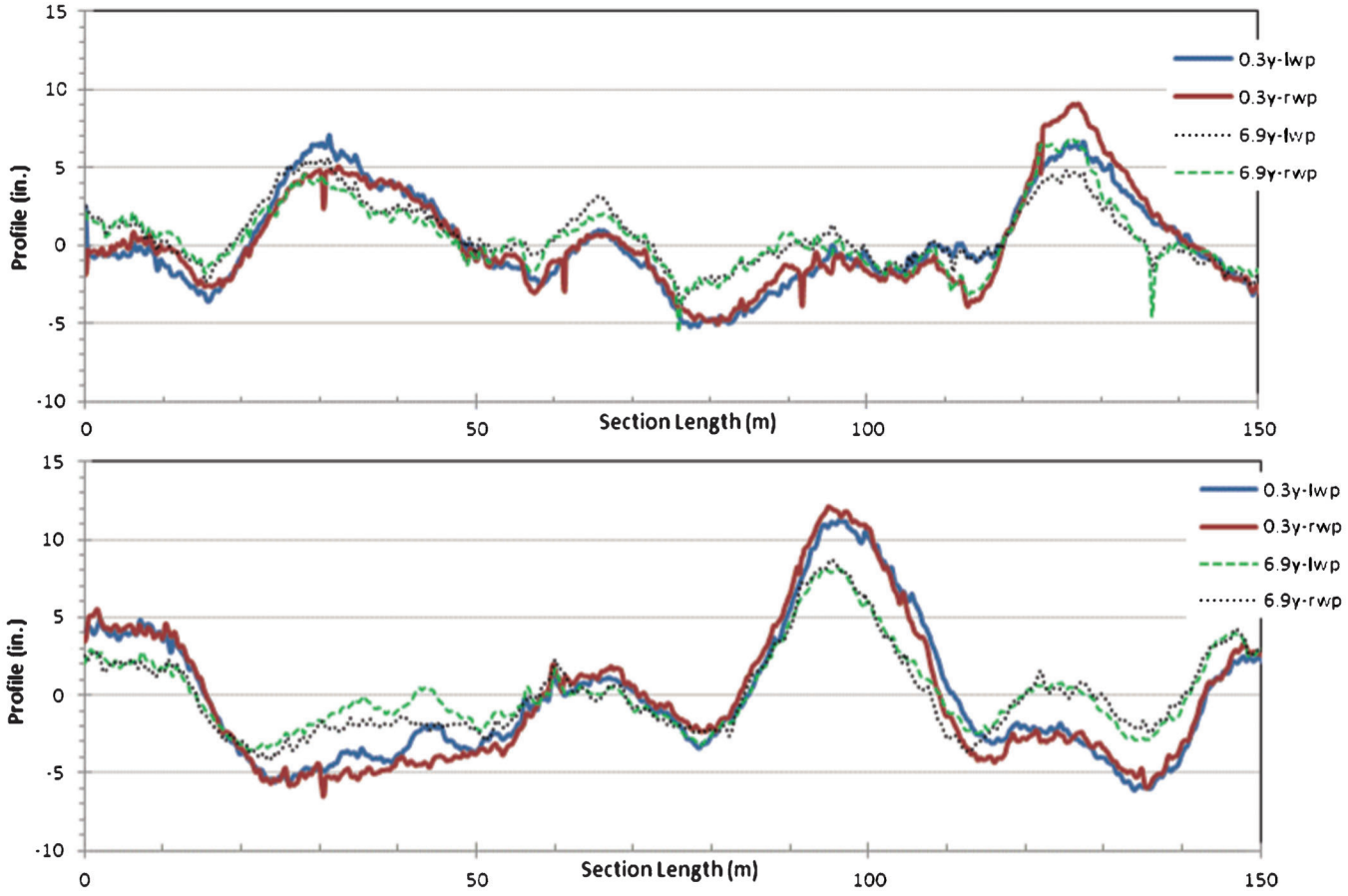

Figure 5.5 Longitudinal profile of Section 1 (top) and Section 2 (bottom).

A final visual inspection was conducted by the researchers at the end of nine years to assess the condition of the pavement. Extensive cracking was observed in all six test sections. Section 5 was by far the worst in terms of crack frequency and severity (transverse, longitudinal and map). This was followed by Section 6. Sections 2 and 3 showed lesser degrees of cracking than all the other sections. These observations were consistent with those reported by the LTPP photographic survey at the end of six years.

6. SUMMARY AND CONCLUSIONS

At the conclusion of the previous study, poor correlation was observed between the predictions made from low-temperature testing (creep compliance and indirect tensile strength) of plant-produced, lab-compacted specimens to the observed field distress obtained from manual surveys. Additionally, tests on recovered binder showed reasonable correlation between observed transverse cracking and expected low-temperature cracking based on BBR and DT testing, in some sections but not all. To investigate this discrepancy further, the current study was initiated to continue long-term monitoring of the study site and to obtain field cores for additional recovered binder testing and mixture compliance testing. The following sections summarize the observations from these additional tests and surveys.

6.1 Layer Thickness and Percent Air Voids

- All test sections showed a further small decrease in layer thickness from the end of the previous study period. A decrease in layer thickness during the lifetime of a pavement is expected due to compaction by vehicular traffic and surface abrasion.
- This reduction in thickness, hence compaction of the layer, is reflected by the decrease in percent air voids (V_a) of the surface layer cores. The drop in V_a was more pronounced between four and 9.5 years after which it leveled off by the end of the 12 years in service. Section 2 (control), which had the lowest V_a (4.5%) at the time of construction, continued to have the lowest V_a and fell below 2% at the end of 9.5 years.

6.2 Binder Test Data

- No changes in the penetration readings of the binders were observed since the end of the previous testing period (four years), indicating that no further aging/stiffening was detected by this test method.
- No change in binder specific gravity (G_b) was observed beyond the initial study period for all binders except for the unmodified binder (PG70-28) and PG64-28 (control) which showed decreases (1.8% and 2.5%, respectively) from the end of the fourth year in service. While this may be attributed to leftover solvent in the binder during recovery process, this supposition was not supported by other binder test data.
- In the case of the unmodified binders, the maximum passing temperature (T_{DSR}) obtained from DSR testing indicated that the binders continued to age up to 12 years of this study, although the aging beyond 9.5 years was minimal.
- The rate of stiffening observed for the unmodified binders was similar, as indicated by the parallel slopes of their regression lines.
- The T_{DSR} of the SBS-modified binder (PG70-28) appeared to be independent of age of the binder.
- The minimum passing temperature (T_{BBR}) of four of the binders increased (became warmer) with age. For the PG58-28 and PG64-28, age did not appear to affect the T_{BBR}, indicating that binder stiffening did not impact the low-temperature cracking resistance of these binders.
- A strong correlation was observed between T_{BBR} and T_{TSAR} of the unmodified binders in this study.
- These data indicate that only Sections 1, 4, 5 and 6 are likely to show thermal cracking in the field at the end of 9.5 years.

6.3 Creep Compliance and Strength Data

- Creep compliance and strength testing of field core samples indicate that all sections will show thermal cracking by the end of 9.5 years.
- The mix with 15% RAP (S4) was slightly stiffer than the corresponding control section (S2) with the same binder grade but no RAP. In terms of critical cracking temperature, the surface mix with RAP might be expected to crack at a temperature 1–2°C warmer than the mix without RAP and the intermediate RAP mix might crack at a temperature 3–4°C warmer.
- Section 3, with the softest binder and low mixture stiffness, is expected to show cracking to a lesser degree.
- The impact of SBS-modification was evident in the low mixture stiffness of the S5 cores and the colder critical cracking temperature.

6.4 Distress Survey Data

- At the end of six years, a photographic survey indicated minimal transverse cracking in Section 3 and the RAP section showed more cracking that the control section. These observations agree well with the low-temperature tests on field cores.
- Section 5 showed the worst performance in terms of thermal cracking susceptibility. While Section 5 was expected to show some cracking based on IDT testing, the severity was not expected to be extreme due to the use of SBS-modification.
- Section 1 (Marshall with AC-20) and Section 6 (Superpave with PG64-16) showed similar cracking intensity, which is consistent with tests on the intermediate layer cores but not the surface layer cores.

6.5 Overall Conclusions

- The recovered binder test results suggest that Sections 1, 4, 5 and 6 would be expected to show transverse

(thermal) cracking in the field at 9.5 years in service. A photographic distress survey at six years did show that these sections had transverse cracking. Section 2 also showed some transverse cracking but it was minimal at the time. The visual distress survey at nine years showed, however, that all sections were exhibiting transverse cracking, though Sections 2 and 3 were performing the best with the least amount of cracking.

- Because of the good correlation between the critical temperatures predicted based on the BBR test results and the TSAR analysis, which uses BBR results plus Direct Tension test results, the additional Direct Tension testing does not appear to be necessary for routine testing purposes, though it may be useful for research.
- The results of testing cores at low temperatures (creep compliance and strength) showed that all sections would be expected to exhibit thermal cracking at 9.5 years. In addition, this testing showed at the RAP mix was slightly stiffer than the control mix and the mix with the softest binder grade had the lowest stiffness. These results are largely as expected and compared well with the field distress.
- The performance of the mix with modified binder in Section 5 is not as expected. Despite a low mixture stiffness and low critical cracking temperature, this section is exhibiting the greatest amount of cracking. The exact reasons for this are unknown.
- With the exception of the mixture with modified binder, then, the observed distress in the field correlates well with the laboratory binder testing and the laboratory tests on field cores.
- The mixture with 15% RAP performed nearly as well as the unmodified control and better than some of the other virgin mixtures under heavy interstate traffic. This suggests that INDOT can continue to use RAP mixtures with confidence.
- The Superpave system has continued to evolve and be refined since this project was constructed. In addition, material suppliers, mix designers and contractors have gained extensive knowledge about working with Superpave. Thus, the performance of Superpave mixes today could be expected to be even better than the performance of these test sections.

REFERENCES

1. McDaniel, R. S., R. B. Leahy, G. A. Huber, J. S. Moulthrop, and T. Ferragut. *The Superpave Mix Design System: Anatomy of a Research Program*. National Cooperative Highway Research Program, Transportation Research Board, Washington, D. C., 2011. Web-only document 186, http://onlinepubs.trb.org/onlinepubs/nchrp/nchrp_W186.pdf
2. Shah, A., and J. Olek. *Development of Indiana's SPS9-A Site*. Publication FHWA/IN/JTRP-2003/17. Joint Transportation Research Program, Indiana Department of Transportation and Purdue University, West Lafayette, Indiana, 2004. doi: 10.5703/1288284313193.
3. Abatech Consulting Engineers. TSAR Software. http://www.abatech.com/TSAR.htm
4. Marasteanu, M. O., and D. A. Anderson. Improved Model for Bitumen Rheological Characterization. Presented at Eurobitume Workshop on Performance Related Properties for Bituminous Binders, Luxembourg, May 1999.
5. Roque, R., and D. R. Hiltunen. A Mechanistic-Based Prediction Model for Thermal Cracking of Asphaltic Concrete Pavements. *AAPT*, Vol. 63, 1994, pp. 81–113.
6. Christensen, R. M. *Theory of Elasticity*. Academic Press, New York, 1992, 145–147.
7. LTPP Products Online. Standard Date Release 24.0 DVD. January 2010. http://www.ltpp-products.com/Default.aspx

APPENDIX

TABLE A.1
Volumetric Properties of Surface Cores t = G Cores (9.5 yr.)

ID	Binder Grade	%AV	%AC	VMA	VFA
S1	AC-20	6.1	6.0	14.3	57.7
S2	PG64-28	1.7	6.9	13.0	86.8
S3	PG58-28	3.8	6.9	13.4	71.8
S4	PG64-28 w/RAP	4.0	7.1	14.8	73.2
S5	PG70-28	5.7	7.0	15.9	63.9
S6	PG64-16	6.3	7.1	16.3	61.3

TABLE A.2
Volumetric Properties of Surface Cores t = H Cores (12 yr.)

ID	Binder Grade	%AV	%AC	VMA	VFA
S1	AC-20	6.5	5.7	14.1	54.0
S2	PG64-28	1.9	7.0	13.5	85.5
S3	PG58-28	4.8	6.5	13.4	64.4
S4	PG64-28 w/RAP	4.6	6.3	13.6	66.1
S5	PG70-28	6.6	6.6	15.9	58.3
S6	PG64-16	6.3	7.1	16.1	61.2

TABLE A.3
Specific Gravity Data of Recovered Binders from Field Cores (All Ages, mo.)

Binder Grade	Tank (0)	t = A (0.5)	t = B (8)	t = C (12)	t = D (18)	t = E (24)	t = F (48)	t = G (114)	t = H (144)
AC-20	1.026	1.034	1.036	1.046	1.047	1.050	1.051	1.046	1.050
PG64-28	1.023	1.031	1.032	1.034	1.041	1.055	1.057	1.033	1.031
PG58-28	1.017	1.024	1.031	1.030	1.033	1.033	1.035	1.040	1.031
PG64-28 w/RAP	1.023	1.031	1.033	1.037	1.039	1.040	1.043	1.035	1.035
PG70-28	0.962	0.994	1.006	1.007	1.013	1.015	1.028	1.018	1.009
PG64-16	1.032	1.038	1.040	1.041	1.041	1.042	1.047	1.039	1.043

TABLE A.4
Penetration (0.1 mm) of Recovered Binders from Field Cores (All Ages) at 5°C

Binder Grade	Tank (0)	t = A (0.5)	t = B (8)	t = C (12)	t = D (18)	t = E (24)	t = F (48)	t = G (114)	t = H (144)
AC-20	26	13	15	8	6	6	6	5	4
PG64-28	36	27	21	19	18	16	16	13	12
PG58-28	53	36	34	25	21	20	21	19	16
PG64-28 w/RAP	36	19	19	13	12	12	12	11	9
PG70-28	56	33	24	15	13	11	10	8	7
PG64-16	16	14	15	11	8	7	8	6	5

TABLE A.5
Penetration (0.1 mm) of Recovered Binders from Field Cores (All Ages) at 25°C

Binder Grade	Tank (0)	t = A (0.5)	t = B (8)	t = C (12)	t = D (18)	t = E (24)	t = F (48)	t = G (114)	t = H (144)
AC-20	89	26	21	20	14	12	11	8	7
PG64-28	79	58	56	42	41	40	40	35	32
PG58-28	124	63	51	51	34	30	31	26	24
PG64-28 w/RAP	79	37	35	27	23	16	17	15	11
PG70-28	68	40	32	20	19	15	15	13	12
PG64-16	31	23	24	12	11	5	6	5	4

TABLE A.6
Results from Indirect Strength Testing of Field Cores (Surface Layer)

ID	Avg. Air Voids, V_a %	Strength, MPa (psi)	Stiffness @ 60 s (GPa)	Cracking Temperature,°C
S1 (AC-20)	7.1	2.67 (386)	41.8	−10.8
S2 (PG64-28)	1.7	3.52 (510)	22.8	−18.9
S3 (PG58-28)	3.7	3.18 (460)	16.9	−22.4
S4 (PG64-28 RAP)	5.4	2.94 (426)	28.4	−17.5
S5 (PG70-28)	5.7	1.89 (275)	15.3	−26.2
S6 (PG64-16)	6.8	2.56 (371)	13.0	−23.0

TABLE A.7
Results from Indirect Strength Testing of Field Cores (Intermediate Layer)

ID	Avg. Air Voids, V_a %	Strength, MPa (psi)	Stiffness @ 60 s (GPa)	Cracking Temperature,°C
S1 (AC-20)	3.4	3.78 (549)	35.9	−16.9
S2 (PG64-28)	2.6	3.88 (563)	25.5	−20.4
S3 (PG58-28)	2.4	3.47 (504)	22.7	−21.9
S4 (PG64-28 RAP)	3.6	3.62 (524)	28.5	−16.2
S5 (PG70-28)	3.0	2.76 (400)	18.8	−23.2
S6 (PG64-16)	5.4	3.44 (499)	29.9	−18.7

TABLE A.8
Transverse Cracking at the End of 3 Years

	No. of Cracks			Length of Crack (m)			
Section (Binder)	Low	Med	High	Low	Med	High	Total Crack Length (m/150 m)
S1 (AC-20)	3.0	0.0	0.0	7.8	0.0	0.0	7.8
S2 (PG64-28)	1.0	0.0	0.0	0.6	0.0	0.0	0.6
S3 (PG58-28)	0.0	0.0	0.0	0.0	0.0	0.0	0.0
S4 (PG64-28 w/ RAP)	0.0	0.0	0.0	0.0	0.0	0.0	0.0
S5 (PG70-28)	14.0	0.0	0.0	36.3	0.0	0.0	36.3
S6 (PG64-16)	3.0	0.0	0.0	11.1	0.0	0.0	11.1

TABLE A.9
Transverse Cracking at the End of 6 Years

Section (Binder)	No. of Cracks			Length of Crack (m)			Total Crack Length (m/150 m)
	Low	Med	High	Low	Med	High	
S1 (AC-20)	7.0	4.0	0.0	18.8	12.9	0.0	31.7
S2 (PG64-28)	9.0	1.0	0.0	8.3	0.8	0.0	9.1
S3 (PG58-28)	1.0	0.0	0.0	0.8	0.0	0.0	0.8
S4 (PG64-28 w/ RAP)	9.0	3.0	0.0	10.2	11.8	0.0	22.0
S5 (PG70-28)	108.0	26.0	0.0	88.8	89.6	0.0	178.4
S6 (PG64-16)	16.0	9.0	0.0	14.2	28.2	0.0	42.4

TABLE A.10
Longitudinal Cracking outside the Wheel Path at the End of 3 and 6 Years

Section (Binder)	Length @ 3 years			Length @ 6 years		
	Low	Med	Total	Low	Med	Total
S1 (AC-20)	233.1	0.0	233.1	130.8	183.0	313.8
S2 (PG64-28)	223.9	0.0	223.9	182.2	125.8	308.0
S3 (PG58-28)	164.5	0.0	164.5	169.0	103.2	272.2
S4 (PG64-28 w/ RAP)	248.7	0.0	248.7	176.6	129.7	306.3
S5 (PG70-28)	288.8	8.5	297.3	77.3	245.2	322.5
S6 (PG64-16)	272.4	27.8	300.2	52.2	257.1	309.3

TABLE A.11
Low Intensity Longitudinal Cracking (m) in the Wheel Path at the End of 6 Years

S1	S2	S3	S4	S5	S6
1.3	1.3	2.0	1.1	64.8	1.0

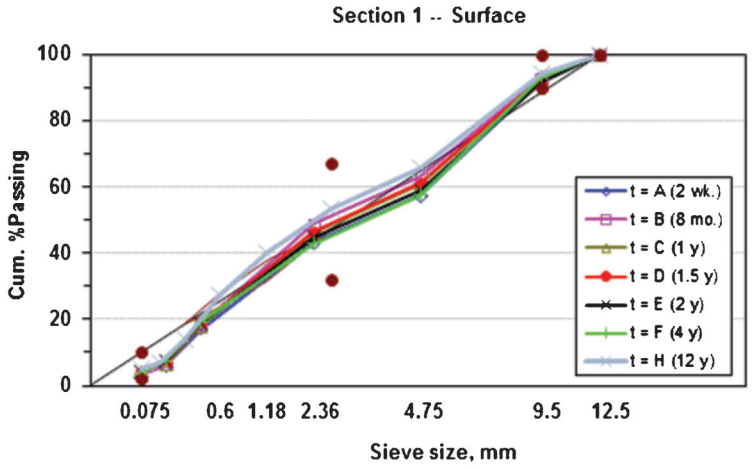

Figure A.1 Gradation of recovered aggregate from Section 1 (AC-20).

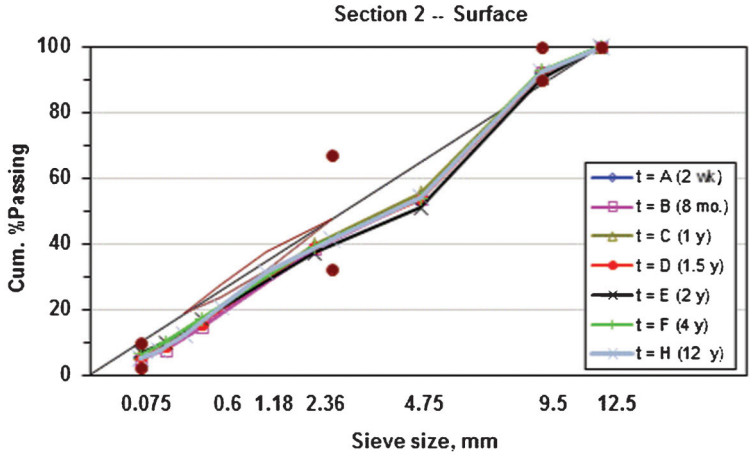

Figure A.2 Gradation of recovered aggregate from Section 2 (PG64-28).

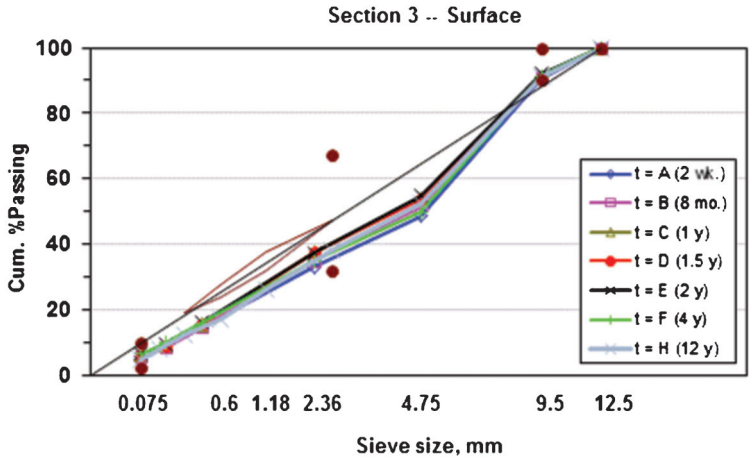

Figure A.3 Gradation of recovered aggregate from Section 3 (PG58-28).

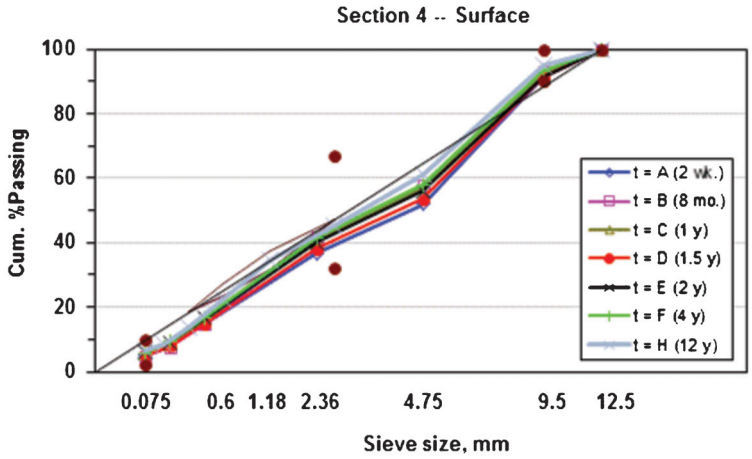

Figure A.4 Gradation of recovered aggregate from Section 4 (PG64-28 w/RAP).

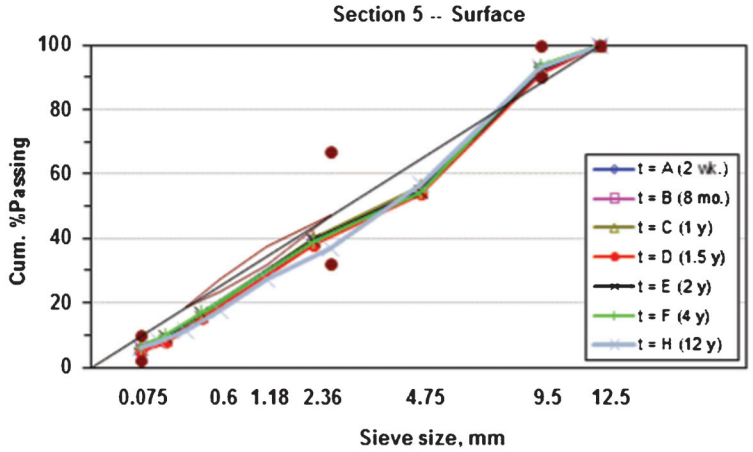

Figure A.5 Gradation of recovered aggregate from Section 5 (PG70-28).

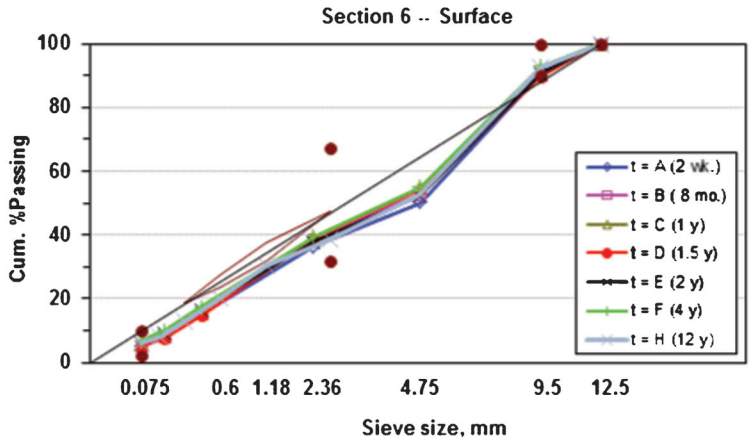

Figure A.6 Gradation of recovered aggregate from Section 6 (PG64-16).

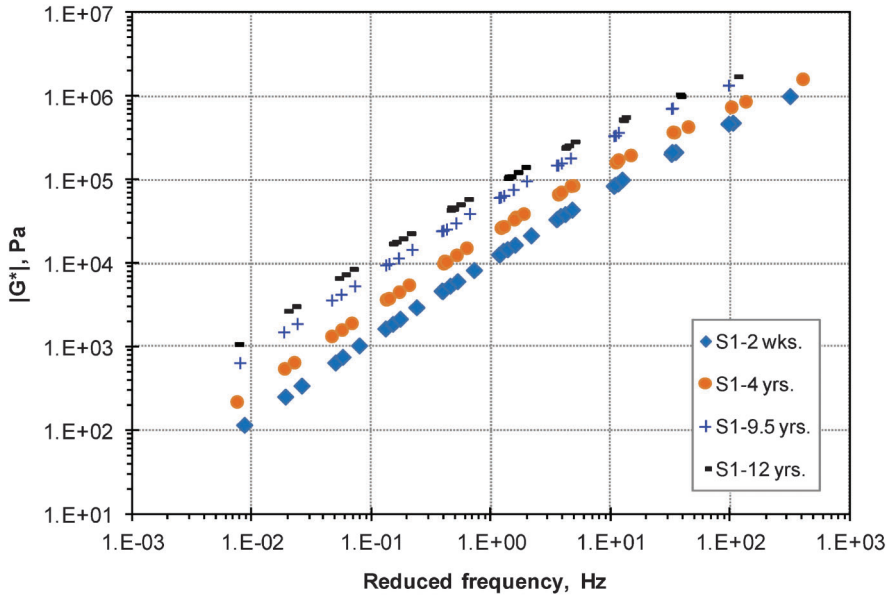

Figure A.7 Master curves for binders recovered from Section 1 (AC-20 =PG64-22).

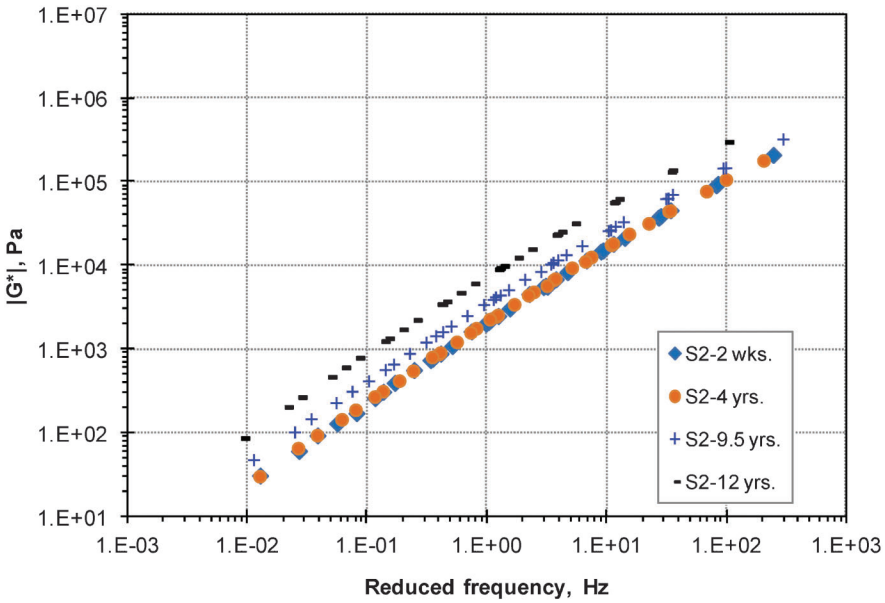

Figure A.8 Master curves for binders recovered from Section 2 (PG64-28).

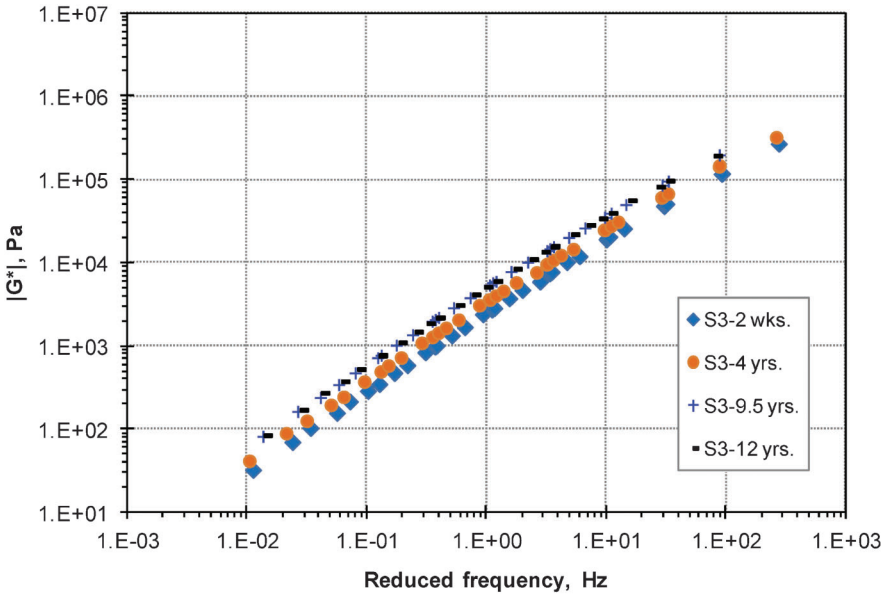

Figure A.9 Master curves for binders recovered from Section 3 (PG58-28).

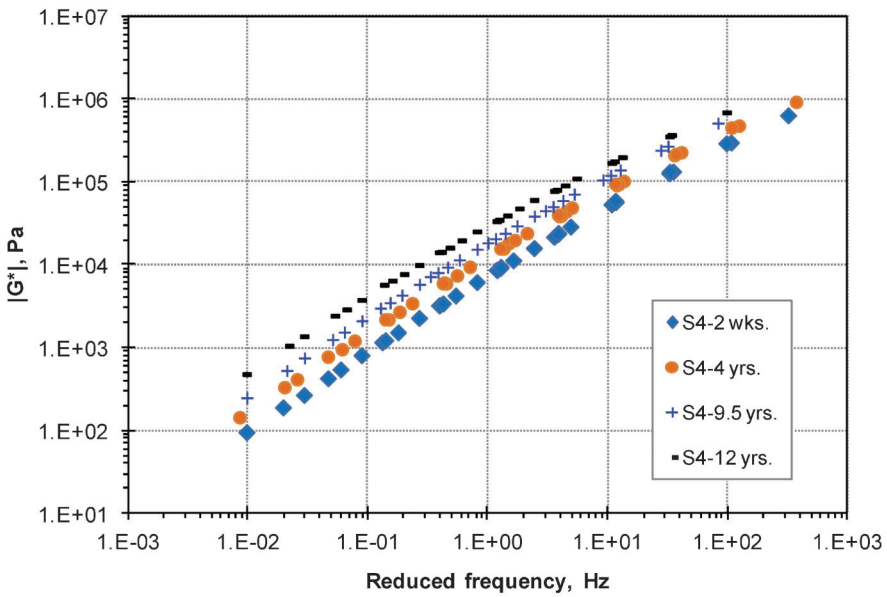

Figure A.10 Master curves for binders recovered from Section 4 (PG64-28 w/RAP).

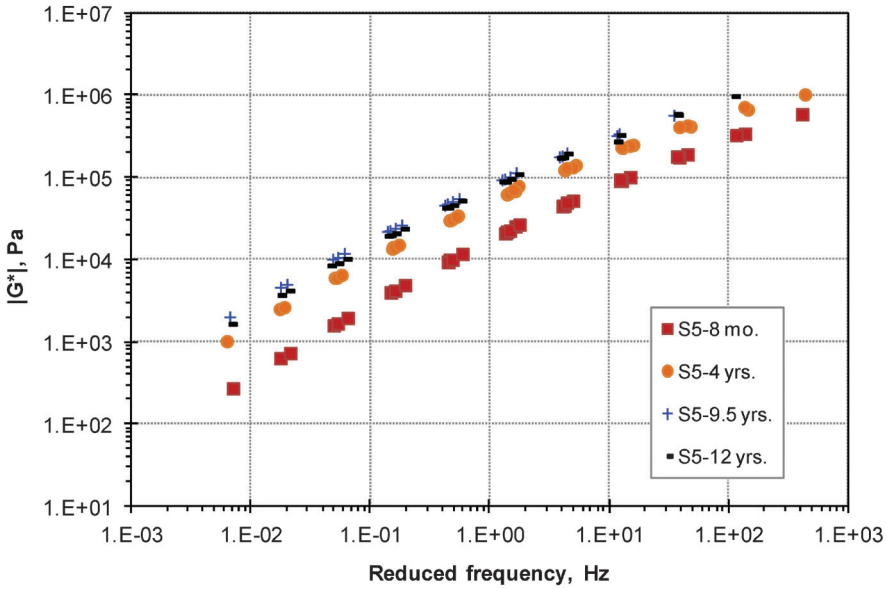

Figure A.11 Master curves for binders recovered from Section 5 (PG70-28).

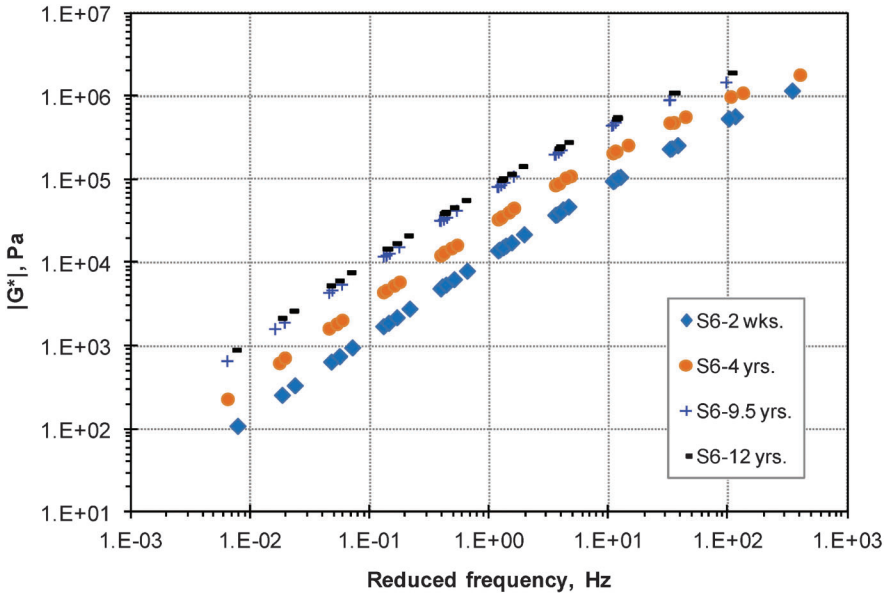

Figure A.12 Master curves for binders recovered from Section 6 (PG64-16).

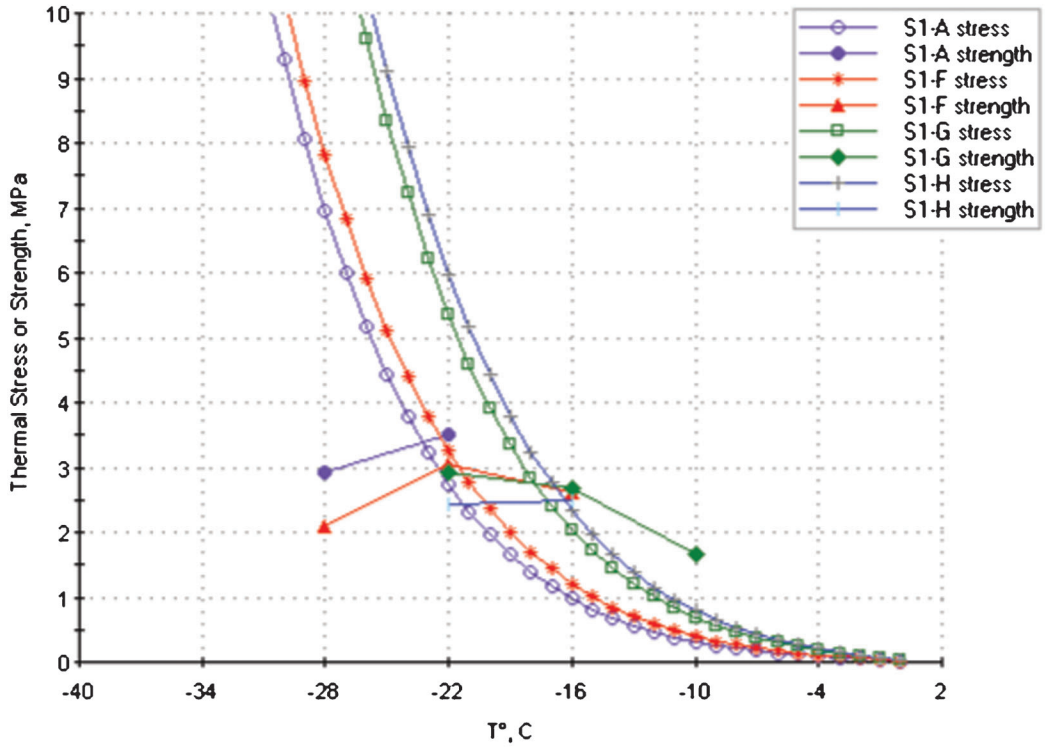

Figure A.13 Thermal stresses in the pavement—Section 1 (AC-20).

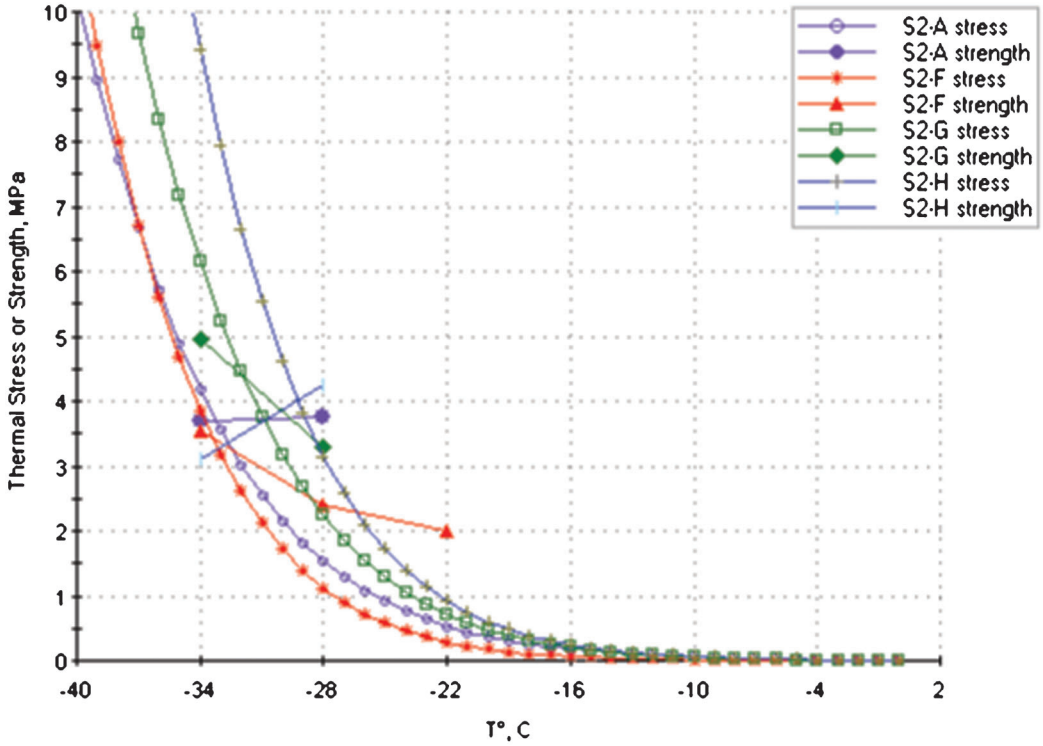

Figure A.14 Thermal stresses in the pavement—Section 2 (PG64-28).

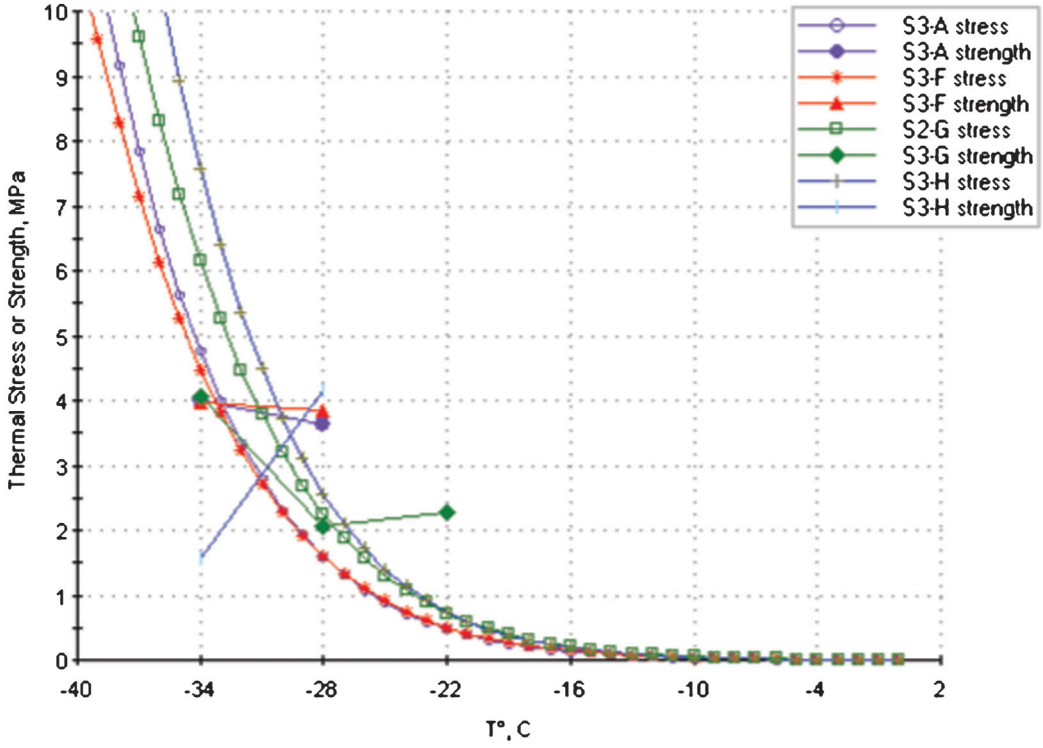

Figure A.15 Thermal stresses in the pavement—Section 3 (PG58-28).

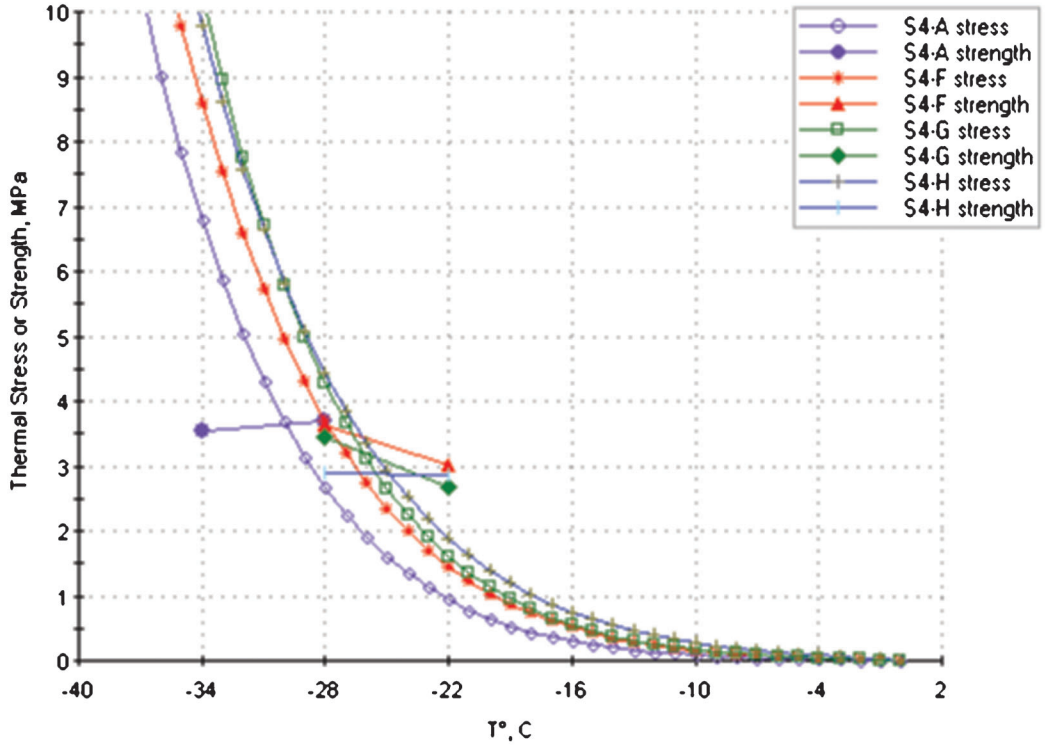

Figure A.16 Thermal stresses in the pavement—Section 4 (PG64-28 w/RAP).

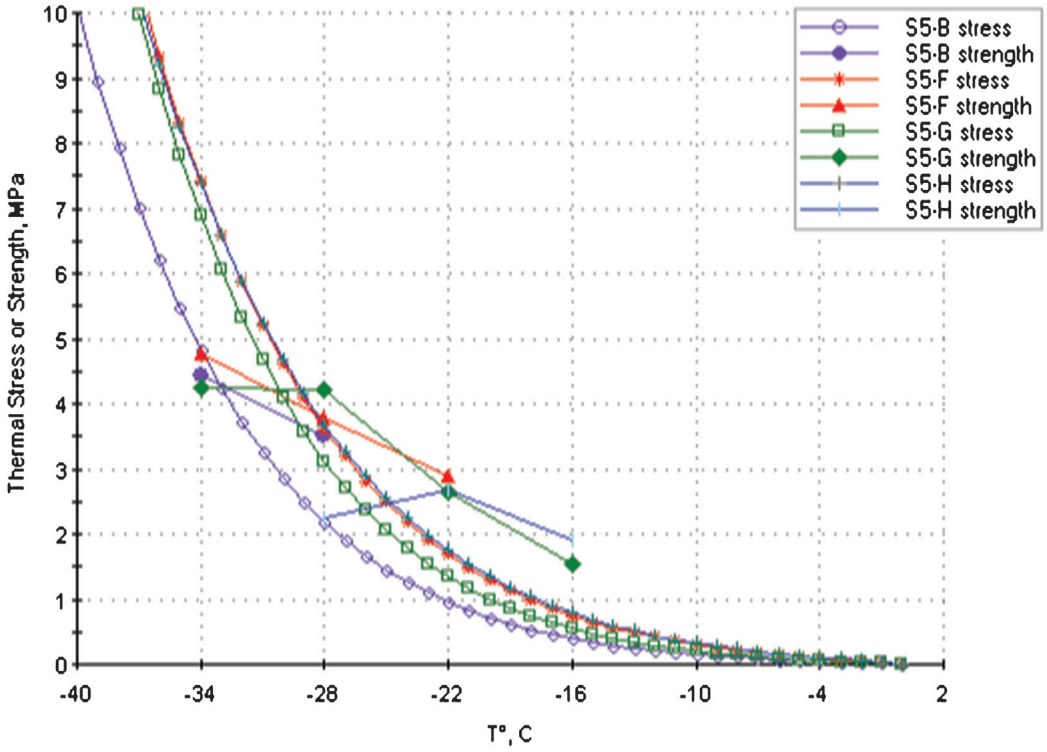

Figure A.17 Thermal stresses in the pavement—Section 5 (PG70-28).

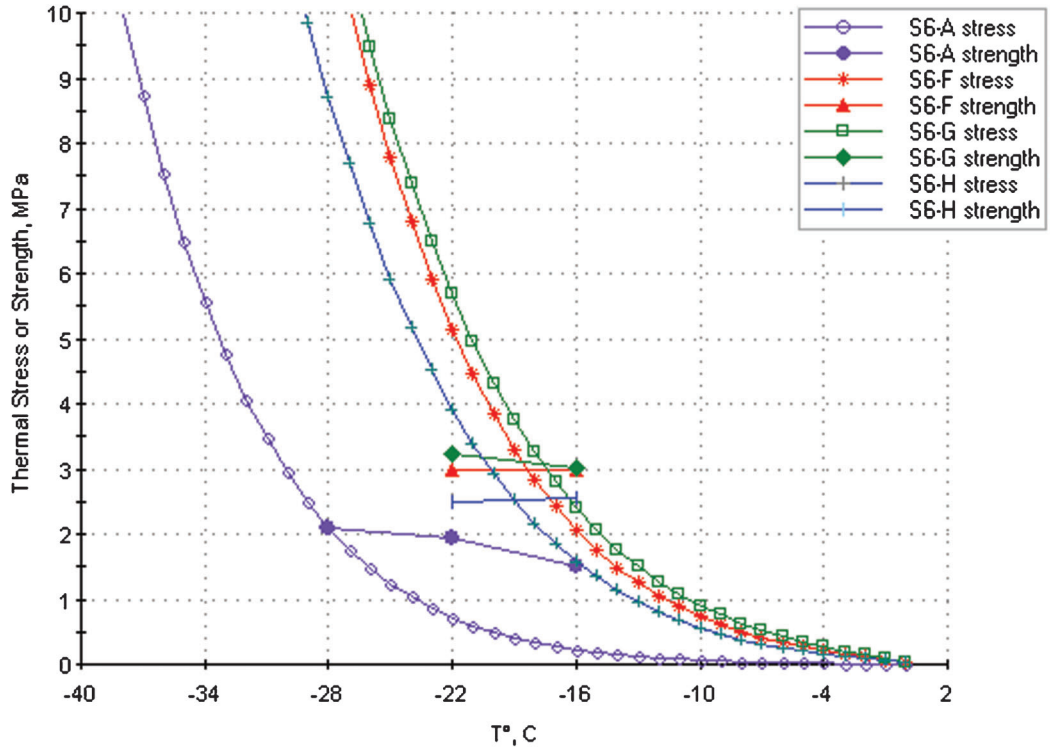

Figure A.18 Thermal stresses in the pavement—Section 6 (PG64-16).

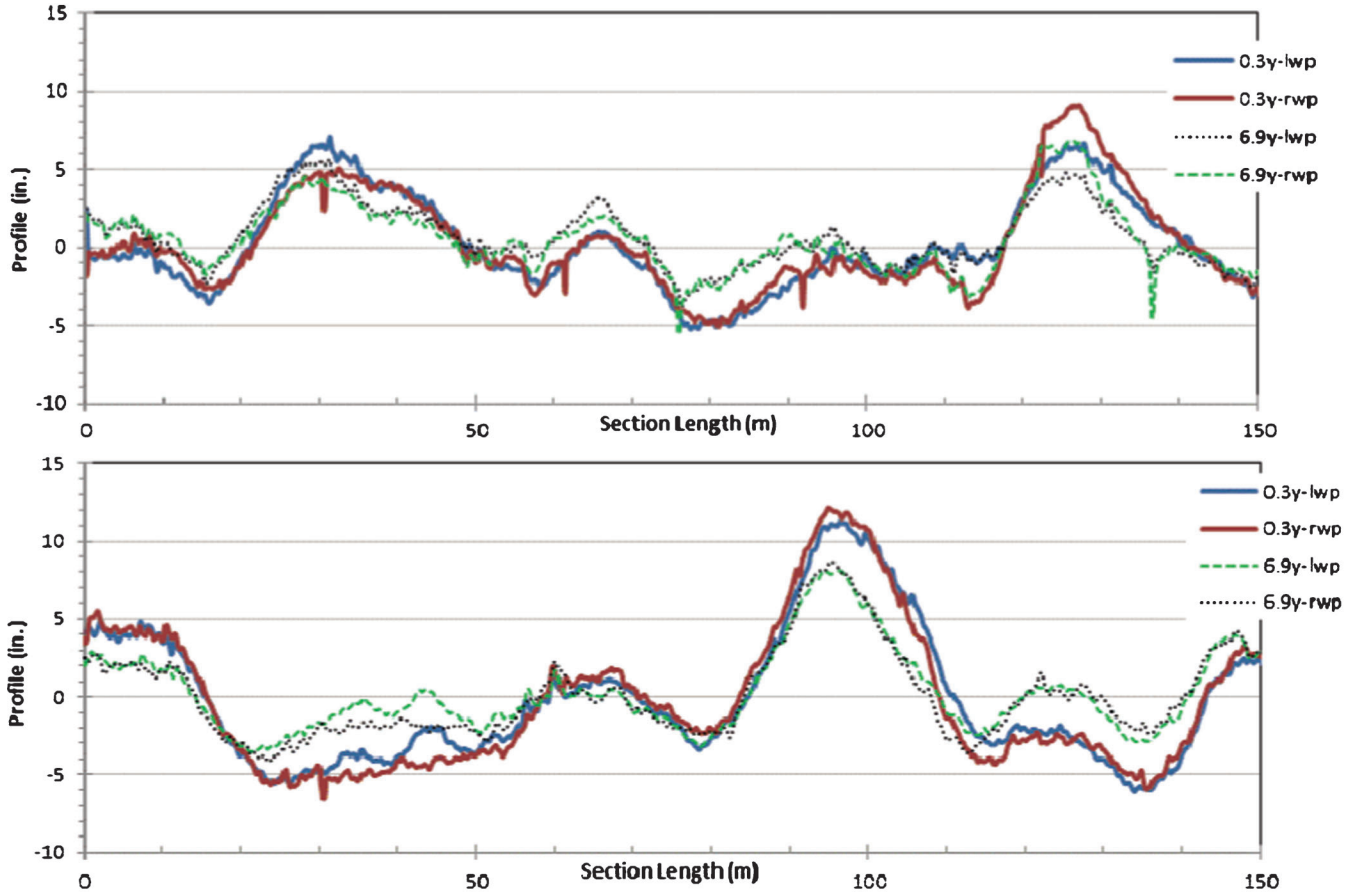

Figure A.19 Longitudinal profile of Section 1 (top) and Section 2 (bottom).

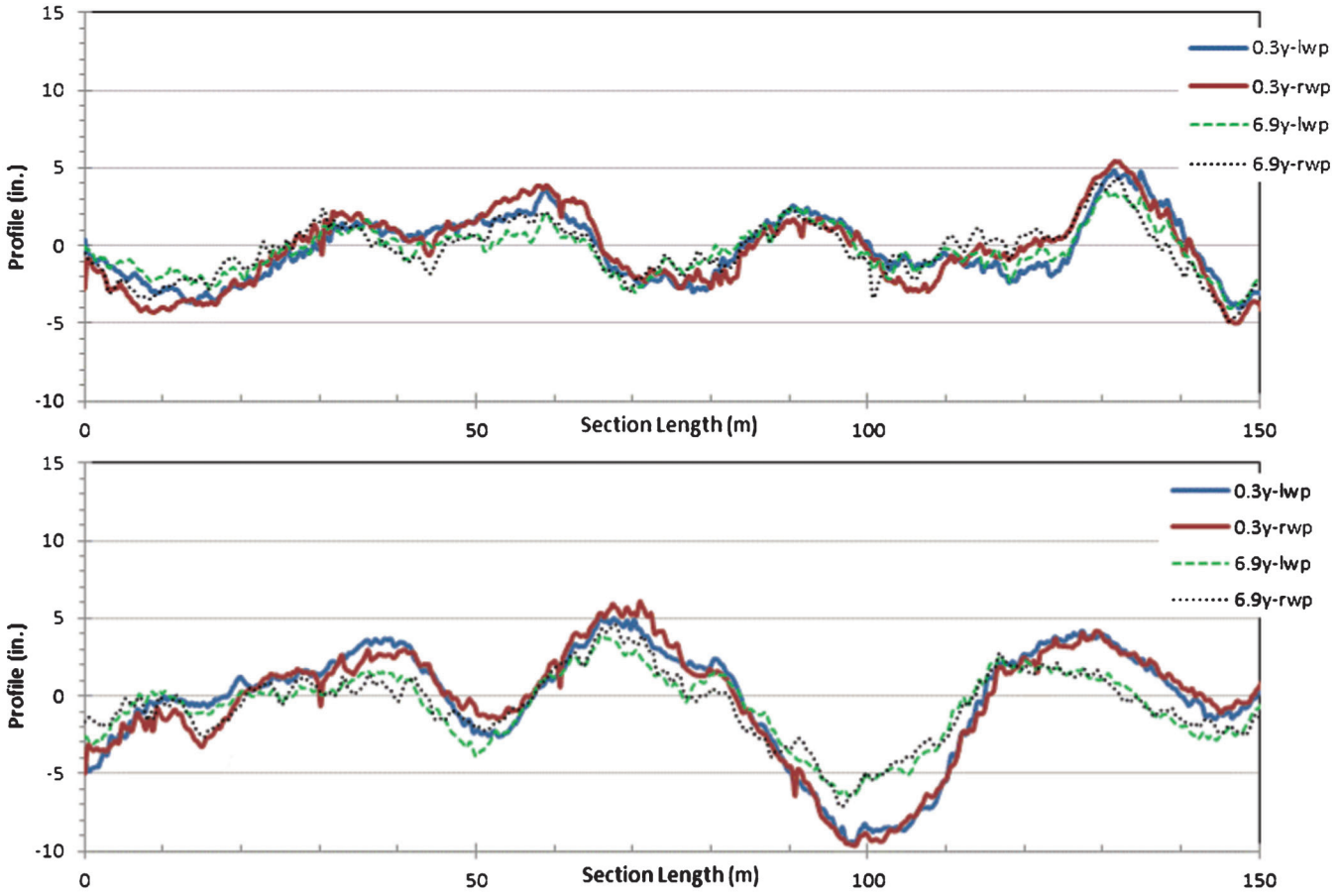

Figure A.20 Longitudinal profile of Section 3 (top) and Section 4 (bottom).

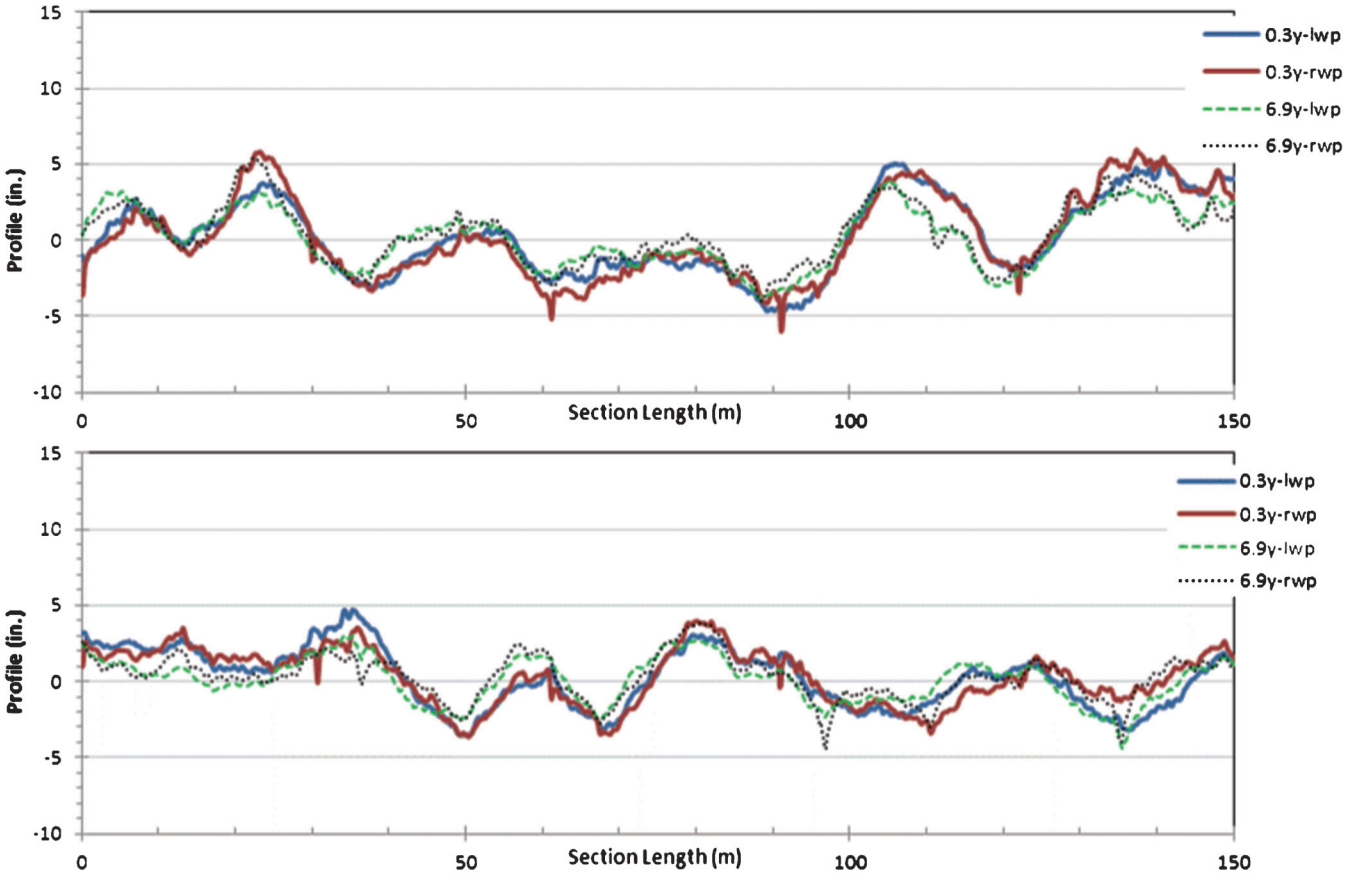

Figure A.21 Longitudinal profile of Section 5 (top) and Section 6 (bottom).